

This is to certify that the

thesis entitled

Seismicity and Tectonics of the Northeastern Sea of Okhotsk

presented by

Cindy Anne McMullen

has been accepted towards fulfillment of the requirements for

M.S. degree in <u>Geological</u> Sciences

Date June 5, 1985

Dr. Kaz Fujita

O-7639

MSU is an Affirmative Action/Equal Opportunity Institution



RETURNING MATERIALS:
Place in book drop to remove this checkout from your record. FINES will be charged if book is returned after the date stamped below.

SEISMICITY AND TECTONICS OF THE NORTHEASTERN SEA OF OKHOTSK

Ву

Cindy Anne McMullen

AN ABSTRACT OF A THESIS

Submitted to
Michigan State University
in pertial fulfilment of the requirements
for the degree of

MASTER OF SCIENCE

Department of Geological Sciences

1985

ABSTRACT

SEISMICITY AND TECTONICS OF THE NORTHEASTERN SEA OF OKHOTSK

Ву

Cindy Anne McMullen

Focal mechanism solutions obtained from P-wave and long-period Rayleigh wave data in the northeastern Sea of Okhotsk region indicate that the southern Cherskiy Mountains are dominated by left-lateral strike-slip motion along northwest-striking fault planes; Shelikov Bay is dominated by thrusting or thrusting with some component of left-lateral strike-slip; and the region north of the Kuril-Aleutian arc-arc junction exhibits oblique thrusting with some left-lateral strike-slip displacement. Compressional axes for most events in the study area trend northeast-southwest.

These fault plane solutions and the distribution of seismicity suggest that there exists a boundary between the Sea of Okhotsk and the North American plate and that the Sea of Okhotsk rotates counterclockwise with respect to the North American plate. Absence of large-scale seismicity along this boundary indicates that relative motion is slow.

ACKNOWLEDGEMENTS

I'd like to express my appreciation to Drs. Kaz Fujita, Bill Cambray, and Mike Velbel for their support and encouragement during these last two years; to Kaz, who managed to convert this geologist from LSU into an earthquake seismologist; to Dr. Cambray, for the Marquette camping trips; and to Mike, for his entertaining stories following mouth-burning Chinese dinners. Special thanks to Norm Sleep, for saving my AGU presentation by producing slides at the last minute. No thanks to Tanya Atwater for asking questions following my AGU talk as I tried to slip out the door.

I'd also like to express my appreciation to the folks at Northwestern University and at the USGS in Menlo Park who allowed access to their station record collections; to Glenn Kroeger for use of the synthetics program; and to Seth Stein, for use of the surface wave program; to the Academy of Sciences, USSR, for copies of the operational bulletin; and to B.M. Koz'min, for his recent book on seismicity of Yakutia.

Many thanks to Tim, Don, Dave, and Soo-Meen, who made those hours spent in the lab all the more bearable; to Dave, for his patience in teaching me the art of working with those elusive events referred to as "microearthquakes"; to Tim, for the drinks at the Peanut Barrel when I should have been writing my thesis; to Soo-Meen, for the introduction to Korean barbeque; and to Don, for making me realize that I don't want to be a Playboy bunny when I grow up. Thanks, Jim, for the Irish music and the opportunity to hang out in your posh San Francisco condo; and thanks Ben, for demonstrating that, even on a student budget, it is possible to enjoy the finer things in life.

This research was funded by an Amoco Graduate Research Assistantship, Michigan State University, and Office of Naval Research contract no. NOO014-83-K-0693.

i

TABLE OF CONTENTS

INTRODUCTION
TECTONIC SETTING
Regional
Northeastern Sea of Okhotsk
SEISMICITY AND FOCAL MECHANISMS
Epicentral Distribution
Southern Cherskiy Mountains
Shelikov Bay to Karaginskiy Island
Karaginskiy Island to Kuril-Aleutian Arc-Arc Junction
DISCUSSION OF RESULTS
TECTONIC IMPLICATIONS
CONCLUSIONS
APPENDIX A: Data analysis techniques
APPENDIX B: Poles of rotation calculations
LIST OF REFERENCES

LIST OF TABLES

1.	Earthquakes for which mechanisms are presented
2.	Epicenters relocated for this study
3.	Kamchatka earthquake mechanisms
B1.	Data set 1 - North Atlantic to 70°N
B2.	Data set 2 - Sakhalin
B3.	Data set 3 - North Atlantic to Sakhalin
B4.	Data set 4 - 68°N to Kuril-Aleutian arc-arc junction
B5.	Data set 5 - North Atlantic to Kuril-Aleutian arc-arc junction 101

LIST OF FIGURES

1	Geographic setting of the Sea of Okhotsk
2	Configuration of the Eurasian, North American and Pacific plates as
	proposed by Chapman and Solomon (1976)
3	Structural elements of the Moma region
4	Structural elements of the Sea of Okhotsk
5	Structural elements along the northeastern Sea of Okhotsk 15
6	Epicentral distribution of the northeastern Sea of Okhotsk
7	P-wave focal mechanism for the event of 1971-05-18
8	Aftershock distribution for the event of 1971-05-18 (after Kozmin et
	al., 1975)
9	Long-period vertical component synthetics for the event of
	1971-05-18
10	Long-period vertical component synthetics at various depths for the
	event of 1971-05-18
11	P-wave focal mechanism for the event of 1970-06-0533

LIST OF FIGURES (cont'd.).

12	Short-period vertical component synthetics for the event of						
	1970-06-05	34					
13	P-wave focal mechanism and Rayleigh wave amplitude radiation pattern	1					
	for the event of 1972-01-13	34					
14	P-wave focal mechanism for the event of 1981-05-22	39					
15	P-wave focal mechanism for the event of 1979-08-19	42					
16	Rayleigh wave amplitude radiation pattern for the event of 1979-08-19	9 43					
17	P-wave focal mechanism for the event of 1978-06-05	45					
18	P-wave focal mechanism for the event of 1972-08-03	48					
19	Rayleigh wave amplitude radiation pattern for the event of 1972-08-03	49					
20	P-wave focal mechanisms for Karaginskiy Island sequence illustrating						
	similar solutions	53					
21	Rayleigh wave amplitude radiation pattern for the event of 1976-01-21	55					
22	Relocation of aftershocks of the Karaginskiy Island sequence	56					
23	Focal mechanisms of events located between Karaginskiy Island and						
	the Kuril-Aleutian arc-arc junction	60					

LIST OF FIGURES (cont'd.).

24 Comparison of the P-wave focal mechanism obtained by Cormier (1							
	and in this study for the event of 1969-12-23						
25	P-wave mechanisms for historic events of northeastern Kamchatka 65						
26	P-wave mechanisms for the events of 1964-11-11 showing their						
	similar solutions						
27	Summary of focal mechanisms along the northeastern Sea of Okhotsk. 70						
28	Proposed plate configurations for the Eurasia and North America plates						
	(from Chapman and Solomon, 1976)						
29	Eurasian - North American plate boundary proposed by this study and						
	a new plate configuration for northeast Asia						
30	Results of poles of rotation calculations						

INTRODUCTION

The Sea of Okhotsk is bounded to the west by Sakhalin and Hokkaido, on the north and northwest by northeast Siberia, on the east by Kamchatka Peninsula, and on the south by the Kuril island arc (Figure 1). The Pacific plate converges in a direction of N60°W and is subducted beneath the Sea of Okhotsk along the Kuril trench. Relative plate motions between the Pacific and North American plates have been obtained by systematic inversion methods by Minster and Jordan (1978). These results indicate that the Pacific plate moves parallel to the far western Aleutian arc but nearly perpendicular to the Kuril arc.

A three-plate configuration of the Eurasian, North American, and Pacific plates has been proposed by Chapman and Solomon (1976) which attributes the Sea of Okhotsk to the North American plate (Figure 2). Using magnetic lineations, the strike of transform faults, and slip vector data from the north Atlantic, the Arctic, and Sakhalin, Minster and Jordan

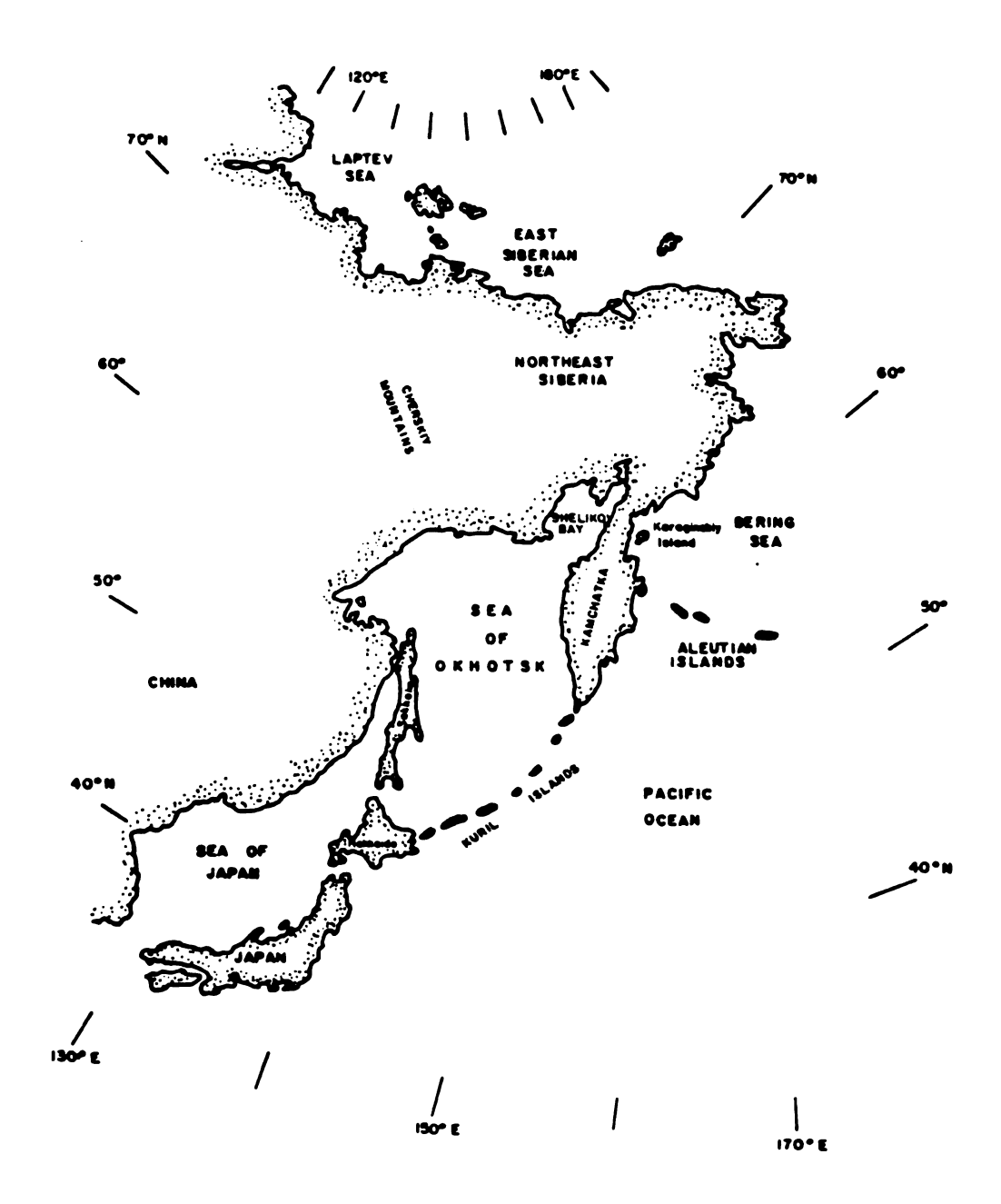


Figure 1: Geographic setting of the Sea of Okhotsk

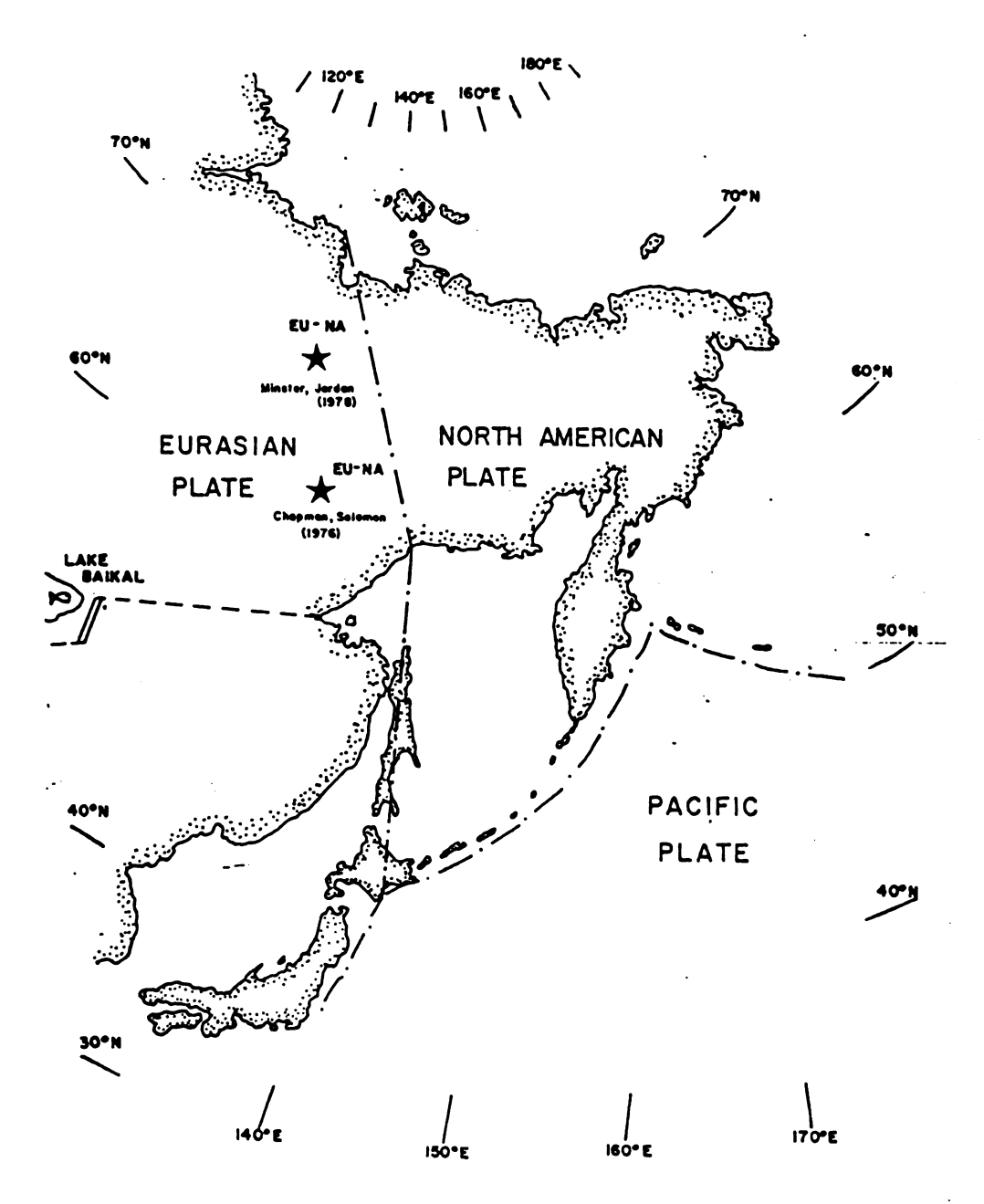


Figure 2: Configuration of the Eurasian, North American, and Pacific plates as proposed by Chapman and Solomon (1976)

(1978) have positioned the Eurasia-North America pole of rotation at 65.85°N, 132.44°E. Chapman and Solomon (1976) have positioned the Eurasia-North America pole at 61.8°N, 130.0°E; the plate configuration preferred by Chapman and Solomon (1976) best fits the tectonics predicted for the Eurasia-North America pole at 61.8°N, 130.0°E.

However, a distinct lineation of moderate-magnitude earthquake epicenters across the northern Sea of Okhotsk region suggests the existence of a plate boundary between the North American plate and the plate containing the Sea of Okhotsk.

The majority of events in the southeastern portion of northeast

Siberia are small earthquakes (Mb ≤ 4.5) detected by Soviet local seismic

networks which operate in this region. There are, however, three

moderate-sized (Mb = 5.3-5.9) earthquakes which align roughly north-south
in the southern Cherskiy Mountains, and five events (Mb = 5.1-5.4) forming
an east-west lineation of epicenters extending from Shelikov Bay (Zaliv

Shelikova) to Karaginskiy Island (Ostrov Karaginskiy) (Figure 1). A zone of
larger earthquakes extends from Karaginskiy Island southward to the

Kuril-Aleutian arc-arc junction. These earthquakes have all occurred
between 1964 and 1983, and are thus relatively recent. Reported depths

indicate that these are all shallow events.

These lineations of moderate to large magnitude earthquake epicenters suggest two alternate plate configurations to the model proposed by Chapman and Solomon (1976). The Sea of Okhotsk may lie within the western portion of the Eurasian plate, or there may exist a separate Okhotsk plate.

The primary objective of this study is to investigate the recent seismicity and tectonics of the northeastern Sea of Okhotsk in order to determine whether a plate boundary exists between the North American plate and the plate containing the Sea of Okhotsk. If the plate boundary exists and can be defined, the relative motion between the two adjacent plates may be estimated using slip vector data obtained from earthquakes in this region.

TECTONIC SETTING

A. Regional

The proposed Eurasia-North America plate boundary in northeastern Siberia lies within the Moma depression, the continental extension of the Arctic Mid-Ocean Ridge (e.g., Chapman and Solomon, 1976; Churkin, 1972; Savostin and Karasik, 1981). The Moma region is a 1200 km long and 100-300 km wide feature which extends southeastward from the Laptev Sea to the upper reaches of the Kolyma River in northeast Siberia (Figure 3).

The Moma rift proper, within the Moma region, is considered the site of the boundary between the continental Eurasian and North American plates; the system of recent faults and tectonic features in the Moma rift zone is most likely the result of the interaction between these two plates (e.g., Chapman and Solomon, 1976; Savostin and Karasik, 1981). The close proximity of the relative pole of rotation between the Eurasian and North American plates calculated by Chapman and Solomon (1976) may account for the structural complexity of the Moma region, since the orientation of stresses varies greatly near the pole of rotation.

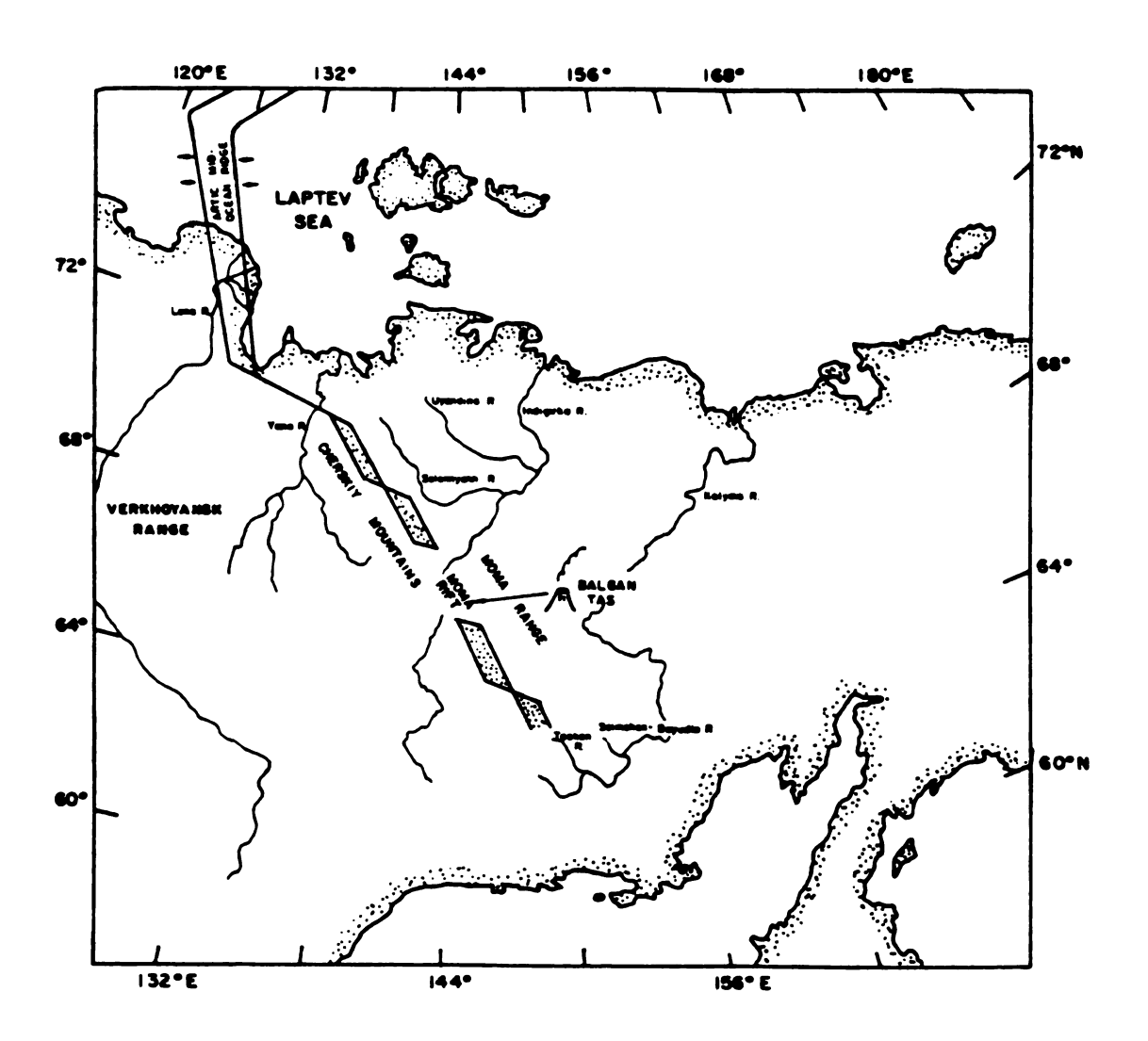


Figure 3: Structural elements of the Moma region

The most prominant structural features of the Moma region include major uplifts and basins. Within the Moma region are two neotectonic structures, the Moma Range and the Cherskiy Mountains, separated by the Oligocene-Quaternary Moma rift. That the Moma region has experienced Neogene tectonic activity is evidenced by manifestations of young volcanism, the presence of thermal springs, and recent seismicity (Afanasenko and Naymark, 1978).

The largest of the depressions within the Moma rift are in the upper reaches of Selennyakh and Uyandina Rivers. These depressions extend southeast almost to the Sea of Okhotsk, including the lower reaches of the Taskan and Seimchan-Buyudin Rivers.

To the west of the Moma rift zone lie the Cherskiy Mountains, within which are many en echelon uplifts which have a predominately northwest orientation. This mountain chain is dissected by narrow graben-like depressions which are often displaced relative to one another. Within the southern Cherskiy Mountains, left-lateral strike-slip faults trend across, but are not traced beyond, the depressions and displace them in a northwesterly direction (Savostin and Karasik, 1981).

The unconsolidated sediments which fill the depressions in the southern Cherskiy Mountains are of Pliocene-Quaternary age, whereas sediments in more northerly depressions along the Moma rift zone are of Oligocene-Miocene age (Savostin and Karasik, 1981). This suggests that the graben-like depressions are younger toward the more southerly regions of the Cherskiy Mountains.

Naymark (1976) suggests that the widespread branching of young faults, as well as the acute intersection of strike-slip faults with grabens in the Cherskiy Mountains, can be attributed to the stress distributions on the crests of young growing uplifts, similar to those observed in the Arabian-African, Rhine, and other rift systems.

Several authors (e.g., Chapman and Solomon, 1976; Savostin et al., 1983; Den and Hotta, 1973) have extended the Eurasia – North America plate boundary in northeast Asia from the Cherskiy Mountains, along the northwestern shore of the Sea of Okhotsk, through Sakhalin and Hokkaido, to the northern Sea of Japan.

The plate boundary through Sakhalin and Hokkaido has been delineated by these authors on the basis of recent seismicity and tectonics of this

region. Sakhalin exhibits a relatively high level of seismicity, including the occurrence of several shallow moderate-sized events. Major structural features such as faults and folds trend northward along the island; displacement along the Central Sakhalin fault, a major north-trending fault through Sakhalin, continues presently (Chapman and Soloman, 1976). The strike of drag folds and second-order faults along the primary north-striking central Sakhalin fault indicates some right-lateral movement along this fault (Chapman and Solomon, 1976).

Sakhalin is also the location of a Mesozoic island arc system along the western margin of Asia (Den and Hotta, 1973; Parfenov at al., 1978).

Although most of the present-day Pacific plate motion is consumed along the Kuril trench, part of this stress may be alleviated along the zone of weakness created by the Mesozoic island arc system.

Near the northern tip of Sakhalin, the seismic belt of Hokkaido and Sakhalin intersects the Baikal-Stanovoi seismic belt, along which a zone of seismicity extends in an east-west direction (Figure 4). Molnar et al. (1973) and Savostin et al. (1983) suggest that the Baikal rift system represents the boundary between a separate Amurian plate and the Eurasian plate; clockwise rotation of the Amurian plate about a pole south of Lake

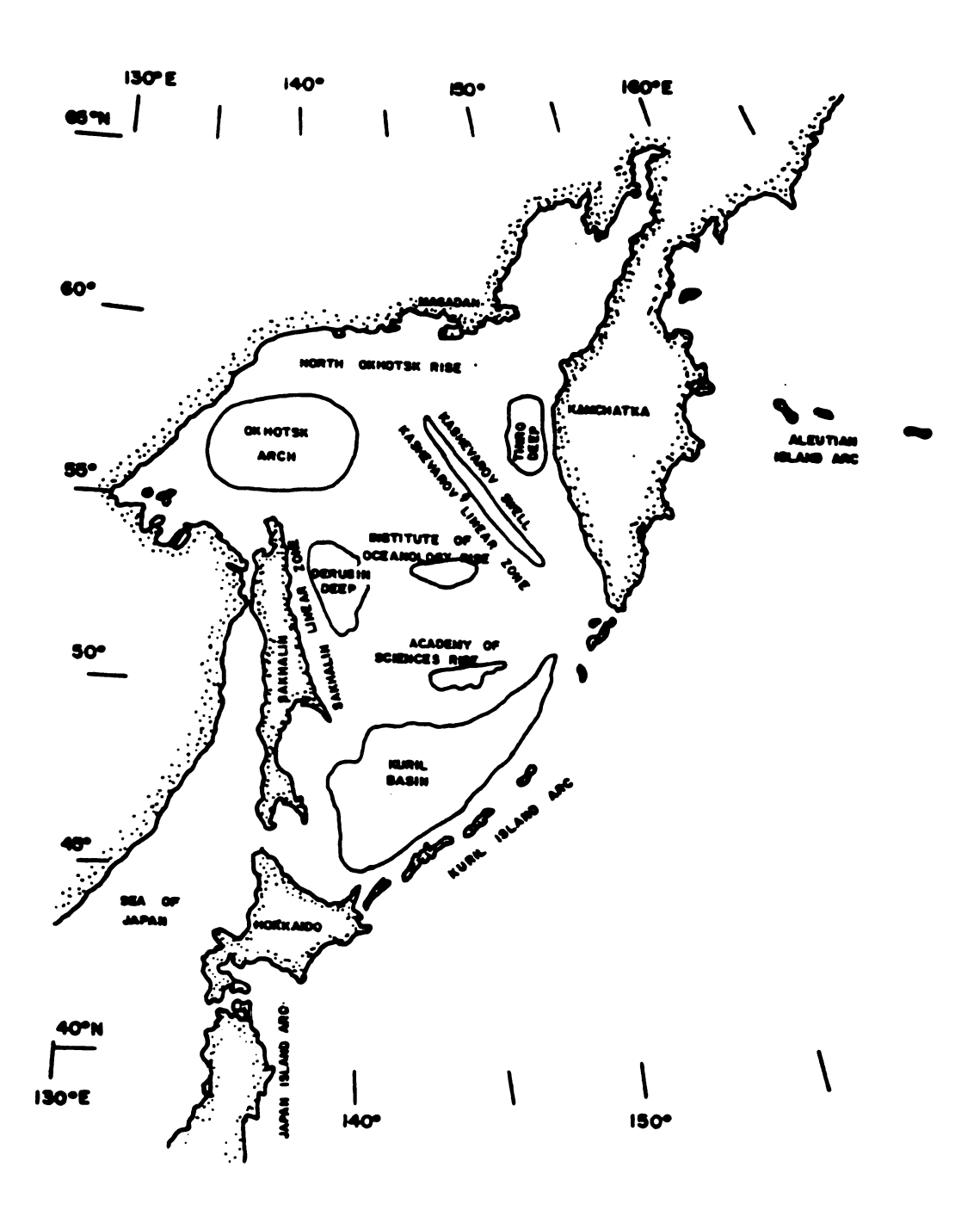


Figure 4: Structural elements of the Sea of Okhotsk

Baikal would account for active extension in the Baikal rift system.

Spreading in this rift system has been limited to a few tens of kilometers since the beginning of Pliocene (Chapman and Solomon, 1976).

whether the plate boundary through Sakhalin extends northward into the southern Cherskiy Mountains is questionable. Distribution of earthquake epicenters in this region is noticeably sparse; only two earthquakes of magnitude greater than Mb = 4.5 (1951-02-12, Mb = 6.0; 1971-09-30, Mb = 5.5) have been recorded within the last 80 years in the region from the northern tip of Sakhalin to the southern Cherskiy Mountains. As the definition of the proposed plate boundary along the western Sea of Okhotsk bears a direct relationship to the associated tectonics of the Sea of Okhotsk and the surrounding lithospheric plates, future studies will be needed in order to gain a better understanding of this region.

Most of the available information of the structural geology of the Sea of Okhotsk has been cited by Savostin et al. (1983). These data indicate that the Sea of Okhotsk may be divided into three zones: a deep, relatively undeformed southern region, a shallow, structurally deformed central region, and a shallow, undeformed northern region. Major structural

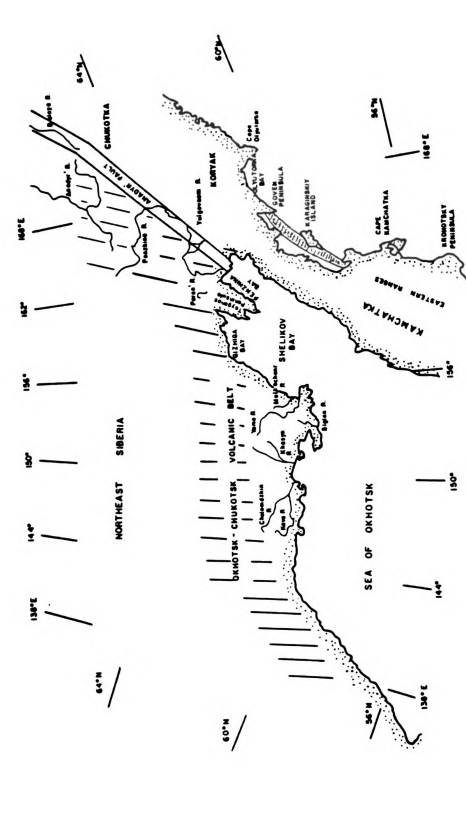
elements within the Sea of Okhotsk include: the Kuril Basin (southern region); the Academy of Sciences rise, Makarov trough, Derugin Deep, Institute of Oceanology rise, Kaschevarov linear zone, Kashevarov swell, Tinro deep, and Sakhalin linear zone (central region); and the North Okhotsk rise (northern region) (Figure 4). A more detailed description of the structural features within the Sea of Okhotsk may be found in Savostin et al. (1983).

The Sea of Okhotsk is bounded to the south and southeast by the Kuril island arc. Normal focus (0-60 km) earthquakes suggest that the Pacific lithospheric slab dips to the northwest at an angle of 20° beneath the Kuril arc. Deep to intermediate-focus earthquakes indicate that the dip angle of the slab increases to 45° at depths of 200 km (Stauder and Mualchin, 1976). Although the deepest recorded seismicity extends to 670 km, analysis of P and PKIKP travel times for intermediate and deep-focus earthquakes suggests penetration of the oceanic slab to depths of at least 900–1000 km (Creager and Jordan, 1984).

B. Northeastern Sea of Okhotsk

The most prominent Mesozoic feature along the northern Sea of Okhotsk is the Late Triassic and Early Cretaceous Okholsk-Chukotsk volcanic belt, which extends as a continuous mountain chain from north of Sakhalin to Chukotka (Figure 5). This zone of andesitic volcanism is believed to have been formed as a result of northward directed subduction of the Sea of Okhotsk beneath northeast Siberia in Aptian through Danian time (Watson and Fujita, 1985).

More recently, a system of local depressions filled with Pliocene and Quaternary sediments, separated by linear or arched uplifts, has developed along the northern edge of the Sea of Okhotsk (Rezanov and Kochetkov, 1962). This zone extends in a continuous band from the northwestern Okhotsk shore through Taygonos peninsula to a system of depressions and uplifts that bound the Koryak region. The magnitude of vertical movements within uplifts of this region during Pliocene–Quaternary time is estimated to be 1000–1200 m, reaching 2000 m in some places (Rezanov and Kochetkov, 1962). This system of depressions can be divided into two regions on the basis of their structural history and the scale of relative



Structural elements along the northeastern Sea of Okhotsk. Shaded region extending from north of Cape Kamchatka to Goven Peninsula is the "sediment-filled linear trough" described by Shapiro (1976). Figure 5:

movement.

The southern region includes a series of depressions confined to the lower reaches of the Siglan, Arman, and Kava Rivers, where downwarping began during Pliocene and has continued until the present (Rezanov and Kochetkov, 1962). Ufimtsev (1975) has described these depressions as "large intermontane basins confined to the largest linear downwarps in mountainous regions which commonly lie at the boundaries of geologic structures of different age".

Depressions within the northern region include the basins of the Chelomdzhin, Khasyn, Malkachanr, and upper Yama Rivers, confined within a region of uplift along the northern shore of the Sea of Okhotsk. There was no sedimentation here in the Pliocene and the depressions did not begin to form until the Quaternary (Rezanov and Kochetkov, 1962); recent tectonic movements began earlier to the south of this region. These northern depressions have been uplifted and are presently being eroded.

This pattern of recent movements is of nearly the same nature on Taygonos Peninsula, which consists of five structurally different zones separated by northeast-striking faults (Leonenko, 1975). Uplifts similar to those found in Taygonos consist of isometric or elongate fault blocks,

forming structural terraces of variable height, separated by grabens (Ufimtsev, 1975).

Also included in this system of depressions and uplifts are Gizhiga Bay and the western portion of Shelikov Bay, although these features developed at a lower elevation and are now submerged below sea level (Rezanov and Kochetkov, 1962).

Similar to the structure of Ghiziga Bay is the depression near Penzhina Bay, the western part of which includes the lower reaches of the Paren' River, and the eastern part which includes the lower reaches of the Penzhina River (Rezanov and Kochetkov, 1962).

The varying intensity and direction of neotectonic movements relative to the Mesozoic structural features of northeast Siberia has resulted in fairly complex structures (Figure 5).

A series of deep fractures extends from Taygonos Peninsula to the junction of the Anadyr' and Belaya Rivers in the Koryak Highlands. These fractures separate the Omolon massif, which accreted to the eastern margin of the Siberian plate in mid-Jurassic time (Fujita and Newberry, 1983), from the deposits of Kamchatka-Koryak (Fujita, 1978). This boundary may be divided into two sectors: Taygonos Peninsula in the south

and the basins of the Penzhina and Anadyr' Rivers in the north.

Two of the fault-bounded structural units of Taygonos Peninsula are interpreted as successive sites of subduction of oceanic crust during Late Permian and Early to Late Cretaceous (Fujita, 1978). In the Penzhina-Anadyr' region, Fujita (1978) also suggests that subduction began in Late Jurassic or Early Cretaceous under an island arc which was eventually accreted onto the continent, with the Anadyr' fault being the suture.

The continental slope of northeastern Kamchatka Peninsula in the region extending from Cape Olyutorka to Cape Kamchatka is exceptionally steep, with inclinations ranging from 10–12°, reaching 25–30° in some places (Yermakov et al., 1975). Off the northeast coast of Kamchatka, the continental shelf is no wider than 30–50 km, locally diminishing to 5–10 km (Shapiro, 1976).

According to Cormier (1975), the last significant deformation of Mesozoic and Tertiary deposits underlying the coastal area of northern Kamchatka was in Middle Miocene through Early Pliocene. Reflection profiles of Scholl et al. (1975) reveal no compressional folding of sediments deposited at the base of the northern Kamchatka margin from late Miocene to Holocene, which is not unusual, since low perpendicular

convergence rates and high depositional rates within a trench favor a subhorizontal floor (Dickinson and Seely, 1979). Fault plane solutions obtained by Cormier (1975), Udias and Stauder (1964), and Stauder and Mualchin (1976) north of the Kuril-Aleutian arc-arc junction indicate that the northeast coast of Kamchatka is still subject to compressive stresses.

On the basis of strong gravity anomalies, Shapiro (1976) has identified a sediment-filled linear trough extending from Cape Kamchatka to Goven peninsula, displaced 150-180 km northwestward from the junction of the Kuril and Aleutian arcs (Figure 5). Shapiro (1976) offers two possible explanations for this linear trough. One such explanation is that the trough may be the northern continuation of the Kuril-Kamchatka trench displaced along a northwest-trending lateral fault passing through the rear of the Aleutian island arc. Shapiro's (1976) preferred hypothesis is that the trough is a northward extension of a depression within the Eastern Ranges of Kamchatka Peninsula. This depression, the Eastern Kamchatka basin, is interpreted by Watson (1985) to represent an Early to Middle Miocene accretionary wedge extending from Kronotsky Peninsula to north of Cape Kamchatka. An alternate possibility is that this sediment-filled linear trough may be a fossil subduction zone which formed as oceanic lithosphere was subducted westward beneath northern

Kamchatka during Late Miocene or Early Pliocene, as subduction along the northeast margin of Kamchatka Peninsula was initiated by back-arc spreading in the Kamchatka Basin during this time period (Scholl et al., 1975; Fujita, 1979).

SEISMICITY AND FOCAL MECHANISMS

Structural features along the northeastern Sea of Okhotsk formed during a period of convergence in the Late Cretaceous (Watson and Fujita, 1985) and do not allow for a recent tectonic interpretation of this region. However, in this study, several focal mechanism solutions have been obtained from recent earthquakes along the northeastern Sea of Okhotsk and have provided a framework to describe present tectonics of the area.

The region under investigation extends from 55 to 65°N and from 140 to 170°E, encompassing parts of northeast Siberia, Kamchatka Peninsula, the Sea of Okhotsk, and the Bering Sea. Regional earthquake epicentral data were obtained through the use of the International Seismological Summary (ISS)(1913–1963), the International Seismological Center (ISC) Regional Catalog of Earthquakes (1964–1982), Rothé (1969), Gutenburg and Richter (1954), annual issues of Zemletryaseniya SSSR (1971–1984) issued by the Academy of Sciences USSR, the Preliminary Determination of Epicenters (1980–1984), and Kondorskaya and Shebalin (1982).

Figure 6 illustrates the epicentral distribution of approximately 1980

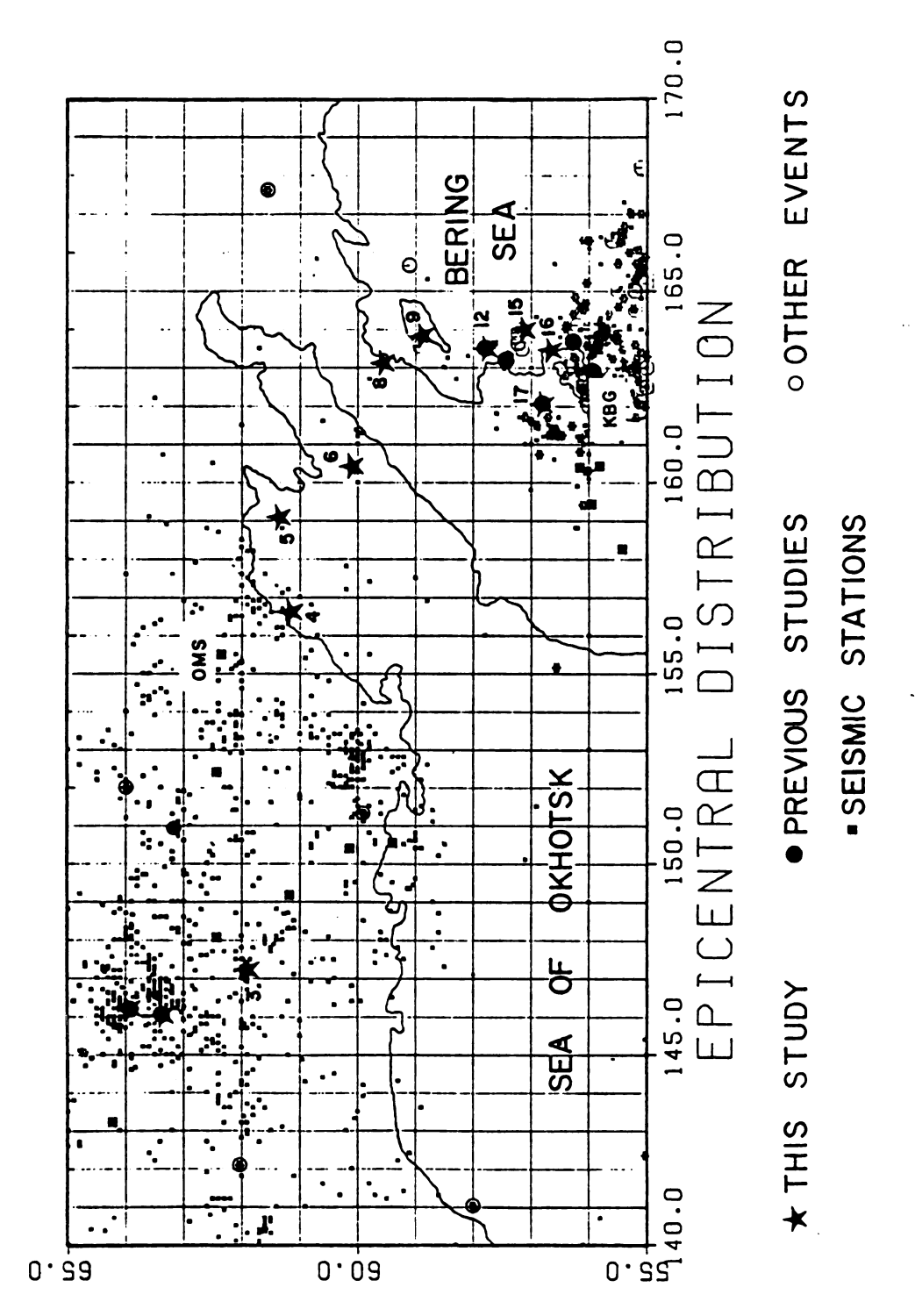


Figure 6: Epicentral distribution of the northeastern Sea of Okhotsk

earthquakes which have occurred in the study area over the past 80 years.

The majority of events in northeast Siberia are of small magnitude (Mb ≤ 4.5) detected only by Soviet local seismic networks. Thirteen of the Soviet seismic recording stations are indicated in figure 6 by small dark squares. Unfortunately, because most of these stations do not usually report to the ISC, first motion data for earthquakes of this study obtained from these local stations were minimal.

The distribution of earthquake epicenters along the northeast coast of the Sea of Okhotsk iand in Shelikov Bay is notably sparse. The absence of seismic stations between Omsukchan (OMS) and Krutoberegovo (KBG) could account in part for the comparatively small number of earthquakes recorded in this region. However, magnitudes of five events in the area from Shelikov Bay to Karaginskiy Island were sufficiently large to record to teleseismically, as were many earthquakes occurring between Karaginskiy Island and the Kuril-Aleutian arc-arc junction. Thus the apparent clusters of the smaller magnitude earthquake epicenters within northeast Siberia and their lack in Shelikov Bay is probably an artifact of station distribution.

There are three notable lineations along which earthquakes of moderate to large magnitude ($5.1 \le Mb \le 7.3$) occur; events along these trends are the primary focus of this investigation. Three moderate (Mb = 5.3 - 5.9) events are aligned north – northwest in the southern Cherskiy Mountains. From northern Shelikov Bay to Karaginskiy Island, five moderate (Mb = 5.1 - 5.4) earthquakes align roughly west–northwest. Within the seismic zone trending southward from Karaginskiy Island to the junction of the Kuril and Aleutian arcs are seventeen shallow–focus events with magnitudes ranging from Mb = 5.4 - 7.3.

Table 1 lists events in the study area for which focal mechanism solutions have been determined. For this study, fault plane solutions were obtained by supplementing first motion polarities read directly from stations records with P-wave data from the ISC Bulletin. With the exception of the three larger events in the southern Cherskiy Mountains, all first motions were read from short-period body waves. Rayleigh wave amplitude radiation patterns were generated for several events which exhibited quality long-period surface waves; when combined with first

Table 1: Earthquakes for which mechanisms are presented

EVE	NT.	DATE	LAT	LONG	DEPTH(km)	MAG(Mb)	STRIKE	DIP	SLIP	STUDIES
1	19	71 - 05-18	63.92N	141.10E	10*	5.9	303	82	2	1,4,8,9,10
2	19	70-06-05	63.26N	146.18E	3*	5.4	316	70	19	1,8,11,12
3	19	72-01-13	61.94N	147.40E	33	5.3	100	88	8	1,8,9,11
4	198	81-05-22	61.09N	156.68E	9**	5.1	278	45	71	1
5	19	79-08-19	61.33N	159.12E	14**	5.1	82	78	14	1,8
6	19	78-06-05	60.09N	160.35E	10**	5.1	306	48	90	1
7	19	75-11-04	60.02N	160.32E	52	4.7	143	33	90	8
8	19	72-08-03	59.51N	163.10E	6	5.2	278	74	340	1
9	19	76-01-21	58.92N	163.55E	7	5.4	210	74	343	1,6,8
10	19	76-01-22	58.92N	163.75E	42	5.2	184	60	352	1
11	19	77-02-17	58.86N	163.87E	18	5.1	188	72	339	1
12	190	69-11-22	57.80N	163.50E	33	6.3	178	19	36	2,3,5,13
13	19	70-06-19	57.45N	163.50E	10	5.2	124	76	0	2
14	190	69-12-23	57.32N	163.10E	33	5.4	33	82	49	1,2,3,13
15	19	45-04-15	57.17N	163.71E	0	6.8	3 56	86	5	1,7
16	19	52-11-30	56.41N	163.15E	0	7.3	176	84	10	1
17a	190	64-11-11	56.63N	161.32E	48	5.3	214	72	31	1
17b	190	64-11-11	56.68N	161.22E	48	5.5	223	60	23	1

- * DEPTH DETERMINED BY MODELLING WAVEFORMS
- ** DEPTH DETERMINED FROM DEPTH PHASES ALL OTHER DEPTHS FROM ISC

EPICENTRAL COORDINATES FROM ISC

STUDIES (mechanism used is first listed)

- 1. THIS STUDY
- 2. ZOBIN AND SIMBIREVA, 1977
- 3. CORMIER, 1975 4. FILSON AND FRASIER, 1972
- 5. STAUDER AND MUALCHIN, 1976
 6. SAVOSTIN ET AL., 1983
 7. AVER YANOVA, 1973

- 8. KOZ'MIN, 1984
- 9. CHAPMAN AND SOLOMON, 1976
- 10. KOZ'MIN, 1973
- 11. SAVOSTIN AND KARASIK, 1981
- 12. KOZ'MIN ET AL., 1975 13. VEITH, 1974

motion data, these patterns proved to be quite effective in constraining orientation of nodal planes. Depths for several events were constrained by reading depth phases and modelling waveforms whenever possible.

A. Southern Cherskiy Mountains

Event 1 (1971-05-18), the largest earthquake recently recorded in the southern Cherskiy Mountains (Mb = 5.9, Ms = 6.6), has been previously studied by Filson and Frasier (1972), Chapman and Solomon (1976), Koz'min (1973,1984), and Savostin and Karasik (1981). Filson and Frasier (1972) analyzed long period surface waves and suggested that the source for this event had a seismic moment of approximately 10**25 dyne-cm. Source propagation for this earthquake was from southeast to northwest over 40 km at 4 - 5 km/sec (Filson and Frasier, 1972).

First motion data obtained from both long and short period body waves clearly indicate a strike-slip mechanism. The nodal planes are fairly well constrained to strike northeast and northwest with a nearly vertical dip (Figure 7), quite similar to mechanisms obtained by previous investigators. Figure 8, after Koz'min et al. (1975), illustrates the distribution of aftershocks for this event. The trend of aftershock epicenters along the northwestern direction indicates that the northwest striking nodal plane is the fault plane. The resultant mechanism implies left-lateral strike-slip faulting along a northwest-striking fault plane.

To further constrain the fault geometry of this event, seven stations

71 MAY 18

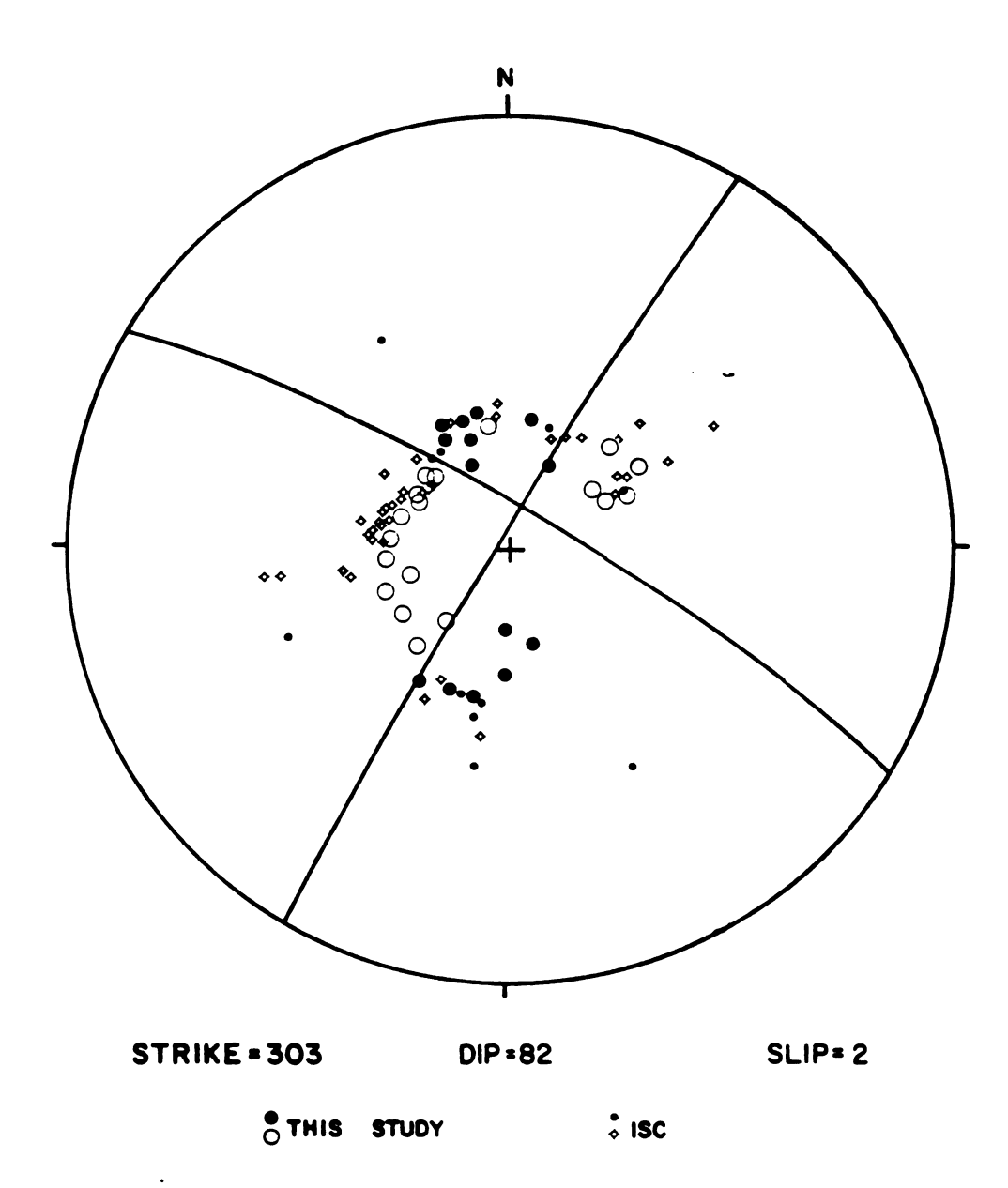
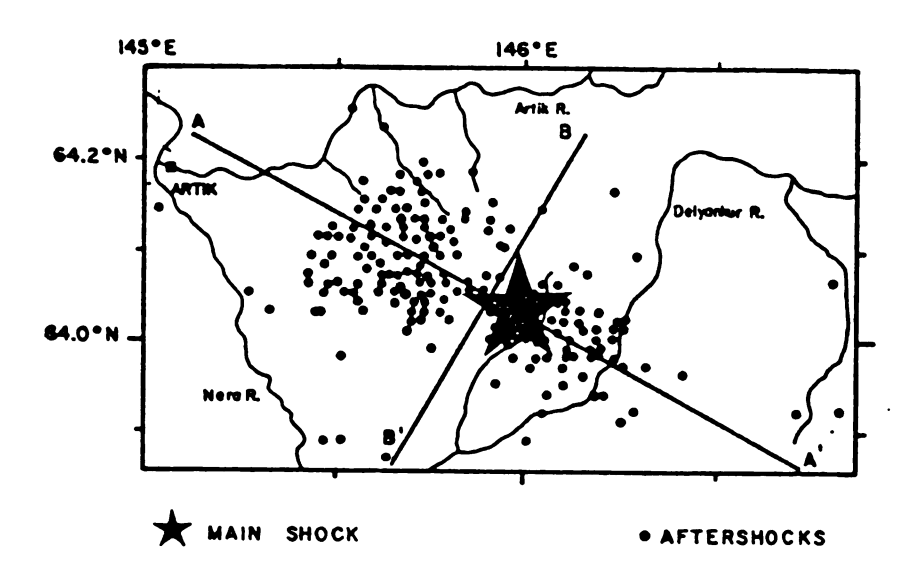


Figure 7: P-wave focal mechanism for the event of 1971-05-18. Compressions are represented by solid circles; dilatations by open circles. Diagram is a lower hemisphere equal area projection.



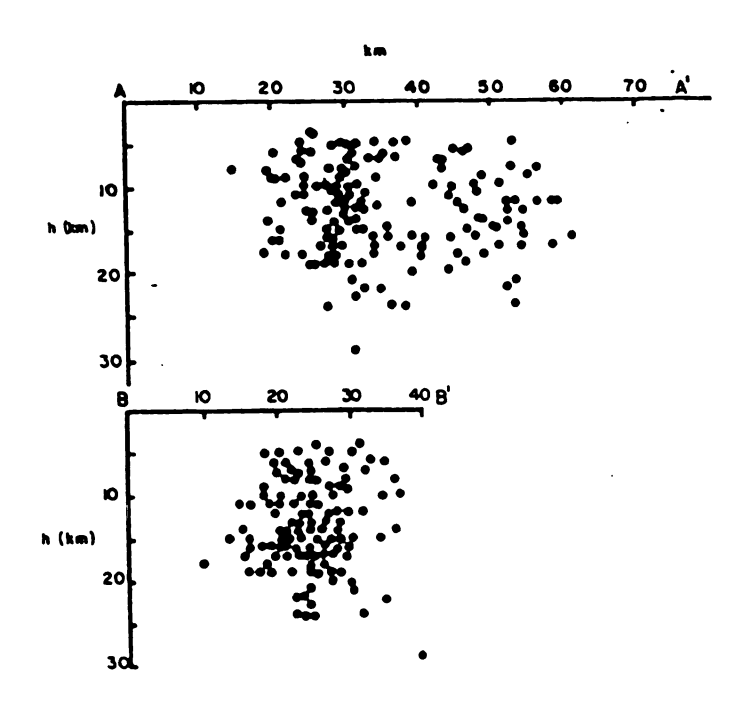


Figure 8: Aftershock distribution for the event of 1971-05-18 (after Koz'min et al., 1978)

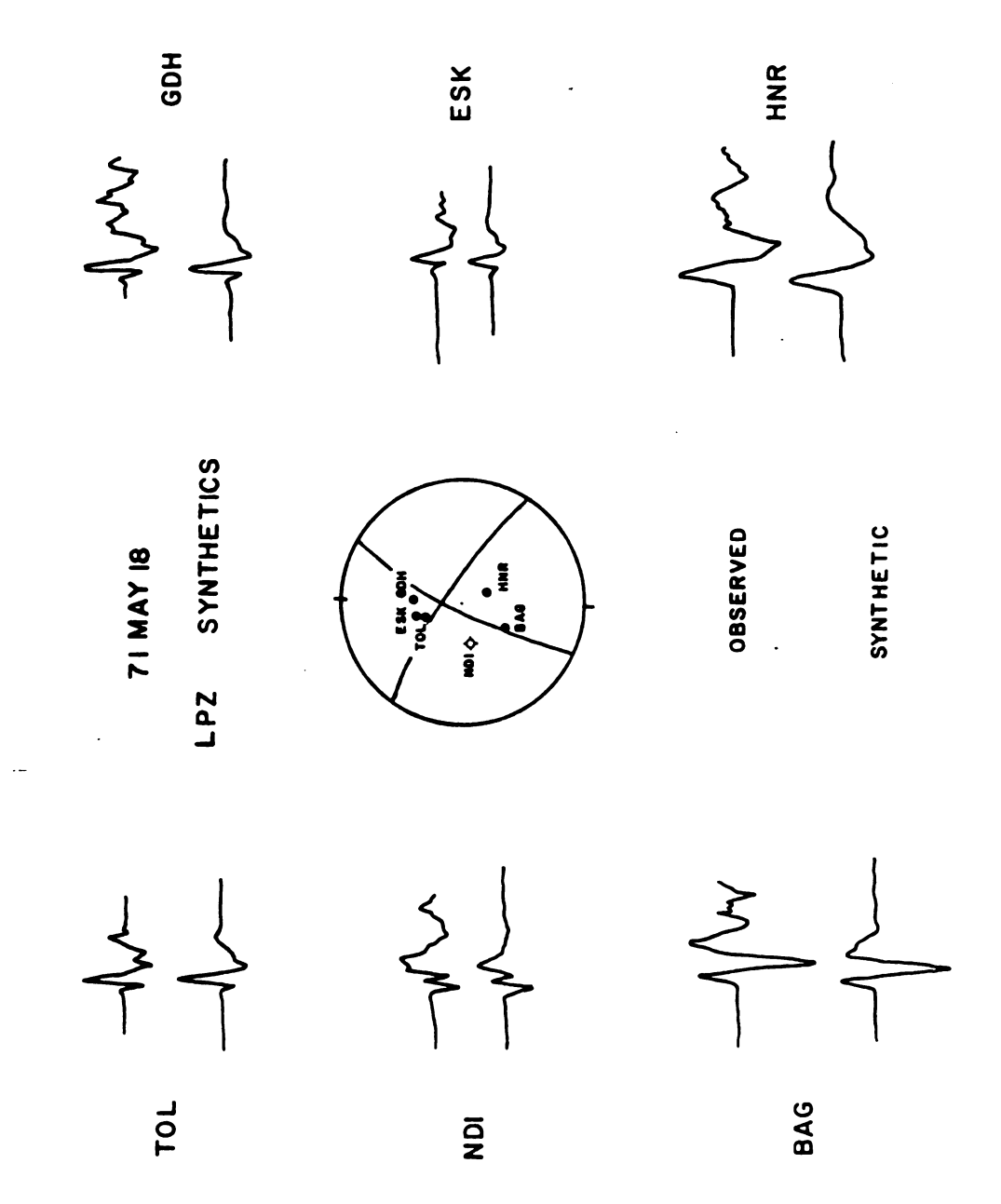


Figure 9: Long-period vertical component synthetics for the event of 1971-05-18. Symbol conventions for P-wave mechanism are identical to those in Figure 7.

71 MAY 18 LPZ SYNTHETICS AT VARIOUS DEPTHS

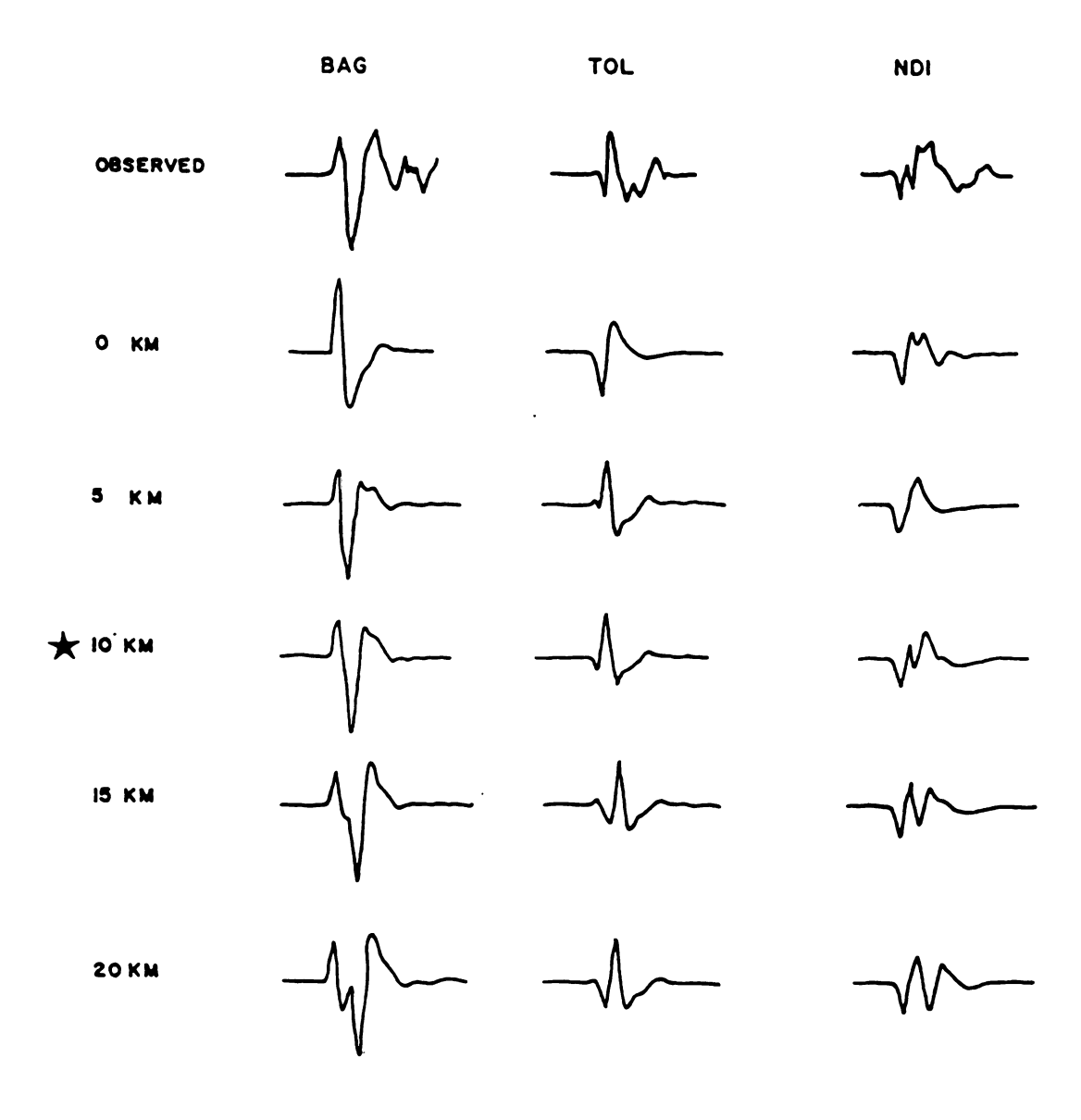


Figure 10: Long-period vertical component synthetics at various depths for the event of 1971-05-18

were used to model long-period body waves using a source-time function of 2,.5,2 sec (Figure 9). More importantly, by varying the depth of the earthquake for various synthetic seismogram traces and observing the arrival time of depth phases, the depth of this event was estimated to be 10 km. Figure 10 shows that a depth of approximately 10 km, as opposed to the depth of 0 km reported in the ISC, best fits the observed data.

Event 2 (1970-06-05), located just south of the previous event, has also been studied by Savostin and Karasik (1981) and Koz'min (1973,1984). The focal mechanism obtained from first motions of short-period body waves for this event were sufficient to constrain the orientation of nodal planes fairly well. The strike of nodal planes for this event are nearly identical to those of event 1 (Figure 11). Note that the strike-slip mechanism for event 2 shows more of a thrust component than event 1.

Modelling of short-period body waves for this event, using seven stations and a comparatively short source-time function of .5, 0, .75 sec, yielded a fault geometry consistent with that obtained from first motion data (Figure 12). Again, waveform modelling proved useful in estimating

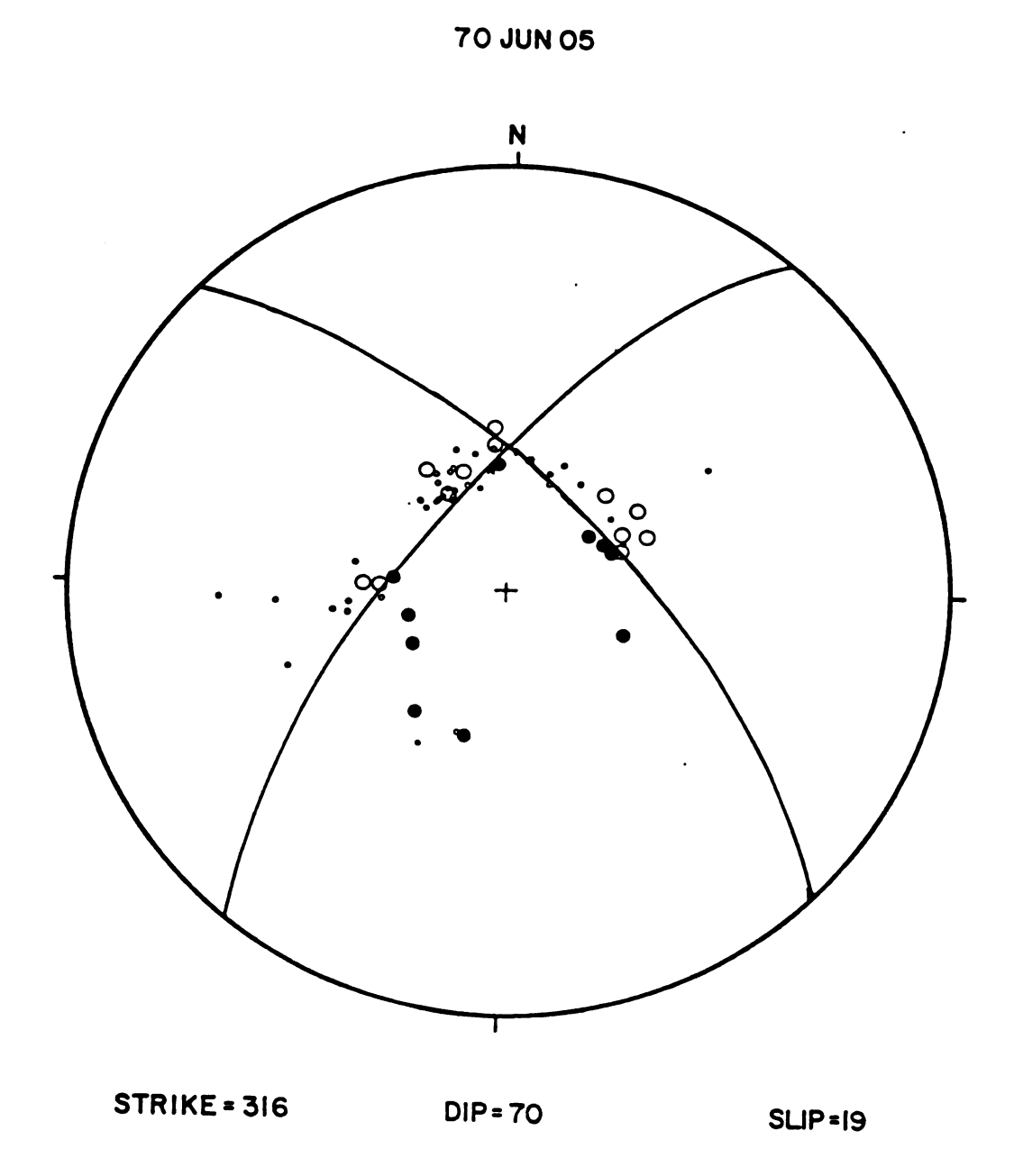


Figure 11: P-wave focal mechanism for the event of 1970-06-05. Symbol conventions used are identical to those in Figure 7.

70 JUN 05 SPZ SYNTHETICS

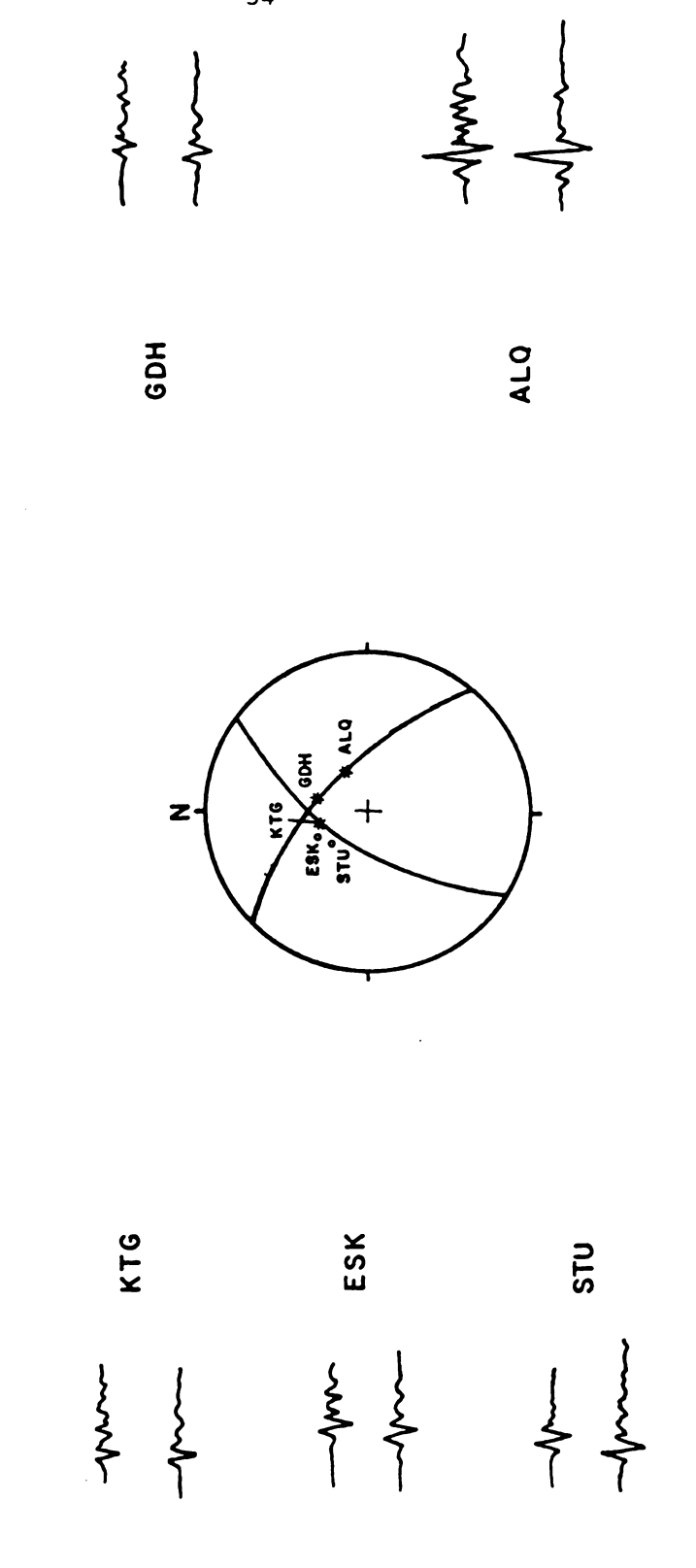


Figure 12: Short-period vertical component synthetics for the event of 1970-06-05. Symbol conventions for P-wave mechanism are identical to those in Figure 7; asterisks represent nodal stations.

the depth of this event at 3 km, compared to the depth of 0 km reported in the ISC.

If the northeast-striking nodal plane is chosen as the fault plane for this event, right-lateral strike-slip faulting is implied. Designation of the northwest-striking nodal plane as the fault plane results in left-lateral strike-slip motion, consistent with the fault geometry of event 1. Thus, on the basis of consistency of fault geometry for events in the southern Cherskiy Mountains and consistency with the northwest oriented strike-slip faults which trend across this region, the northwest-striking fault plane is chosen as the fault plane for event 2.

The southernmost event studied in the southern Cherskiy Mountains, event 3 (1972-01-13) lies southeast of the previous two events. The poor quality of both long- and short-period body waves for this earthquake did not permit modelling of waveforms. This event did, however, exhibit excellent surface waves, enabling the generation of the Rayleigh wave radiation pattern illustrated in figure 13. A well-distributed azimuthal coverage using seventeen stations yielded a pattern consistent with short-period first motion data indicating a strike-slip solution along an east-west direction with a small component of thrust. The mechanism

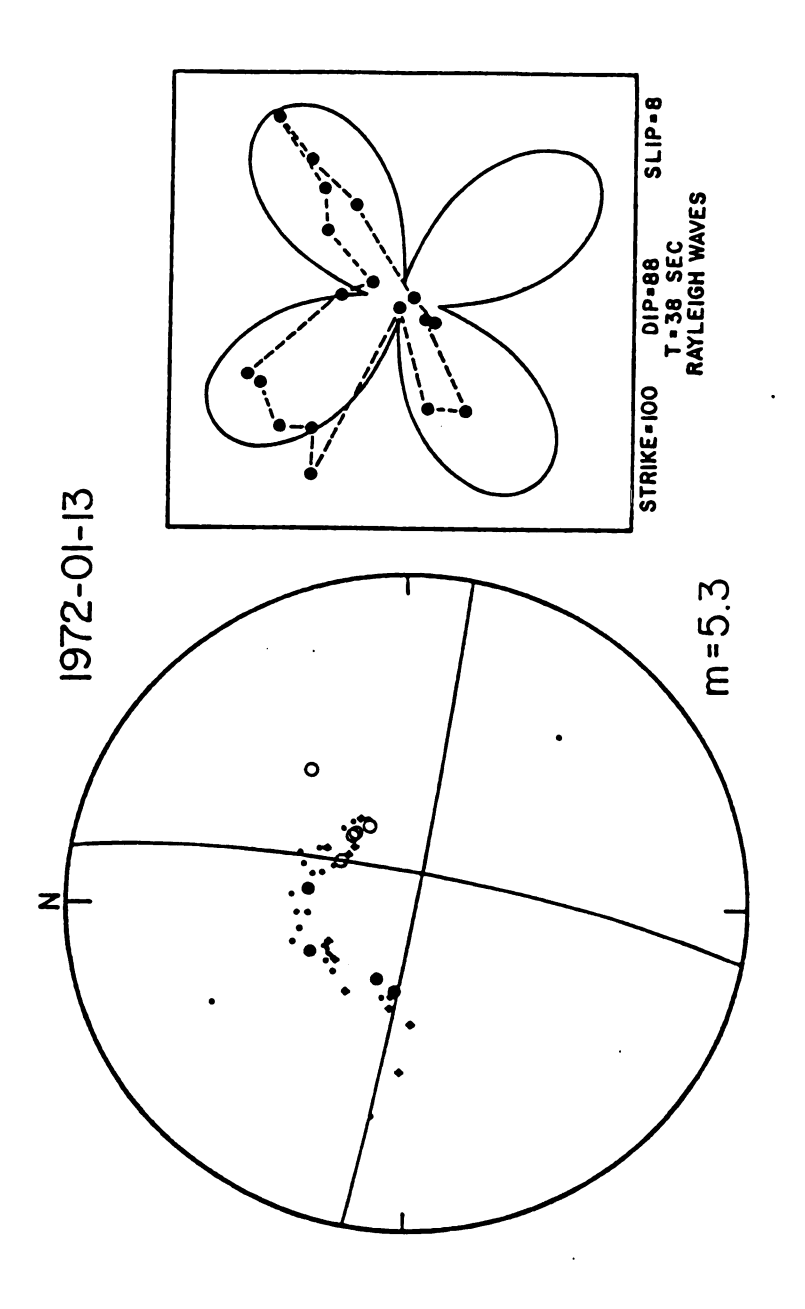


Figure 13: P-wave focal mechanism and Rayleigh wave amplitude radiation pattern for the event of 1972-01-13. For P-wave mechanism, symbol conventions are identical to those in Figure 7. For Rayleigh pattern, solid circles represent data points; curved lines represent theoretical radiation pattern for this particular fault geometry.

obtained from this Rayleigh pattern differs slightly from the solution obtained by Chapman and Solomon (1976) and Savostin and Karask (1981), whose solutions show a more northwest and northeast orientation of nodal planes. Because the solution in this study was obtained by combining short-period P-wave data with long-period Rayleigh radiation patterns, this solution is considered to be better constrained and is thus preferred over the solutions of Chapman and Solomon (1976) and Savostin and Karasik (1981), who used only P-wave data to derive a mechanism for this event.

The northwest-striking nodal plane was designated as the fault plane, consistent with regional structure and solutions obtained for the previous two events in the southern Cherskiy Mountains.

Analysis of Rayleigh wave spectral amplitudes also provided estimates of the seismic moment of this earthquake of about 5.6 x 10**24 dyne-cm.

Thus the three events studied in the southern Cherskiy Mountains are characterized by left-lateral strike-slip along a northwesterly striking fault plane. Orientation of compressive stress axes for all three events in the southern Cherskiy Mountains are in a northeast-southwest direction.

B. Shelikov Bay to Karaginskiy Island

Epicenters for three moderate-sized (Mb = 5.1) events located in Shelikov Bay form a nearly east-west lineation along the northeastern shores of the Sea of Okhotsk.

The westernmost earthquake, event 4 (1981-05-22), occurred along the western shores of Gizhiga Bay. Good depth phases recorded at four stations for this event indicate a relatively shallow focal depth of 9 km. The moderate magnitude of 5.1 for this event resulted in a mechanism whose solution was constrained using short-period first motion data only (Figure 14). Fourteen first motions read directly from WWSSN records of stations recording this event were supplemented with first motions reported in the ISC, as well as first motion polarities reported in the Soviet operational bulletin.

Soviet first motion data were important in attempting to constrain this mechanism, since the relatively small epicentral distances of those stations from the earthquake projects the station near the perimeter of the focal sphere. Travel-time residuals for the Russian stations Yakutsk (YAK) and Susuman (SUUS) were considered anamalously high (4.6 and 12.9)

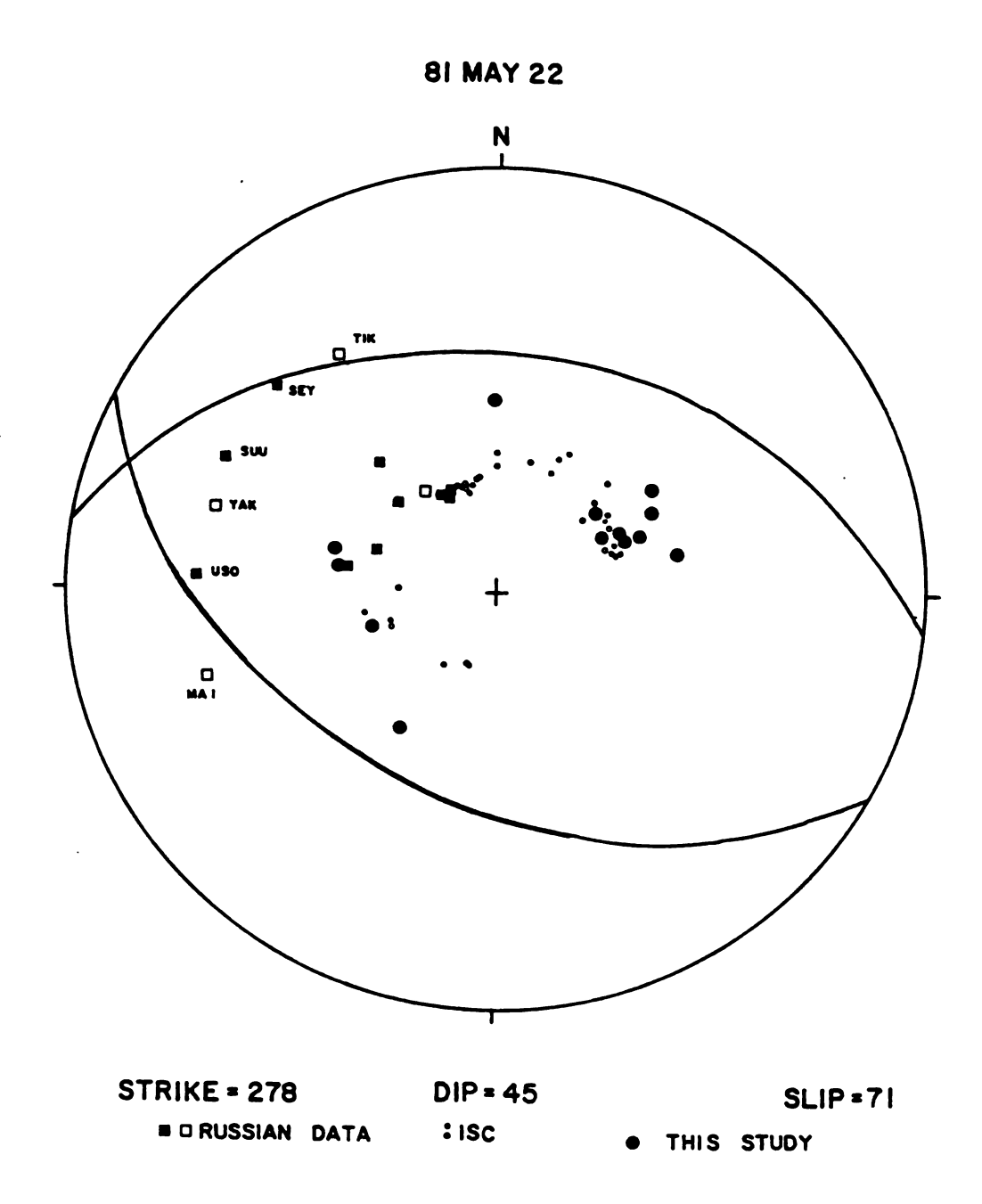


Figure 14: P-wave focal mechanism for the event of 1981-05-22. Symbol conventions used are identical to those in Figure 7.

s, respectively) and consequently were not considered reliable first motion data for this event. Stations Tiksi (TIK), Seymchan (SEY), Ust'Omchug (USO), and Magadan 1 (MA1) had low residuals and were considered reliable. The lower focal sphere projections of these stations and their reported first motions are identified in Figure 14.

Critical to this mechanism are the dilatations reported at the two Russian stations MA1 and TIK, as all first motions read directly from WWSSN records are compressions. This event is clearly a thrust fault with moderately dipping nodal planes. If stations SEY, USO, and SUUS are considered reliable (residuals for these stations are acceptable) the nodal planes for this event strike east-west since it is quite probable that the dilatation reported at YAK may be erroneous.

The northward dipping nodal plane is fairly well constrained by the two stations TIK and SEY. The exact orientation of the other nodal plane is less certain; the two stations MA1 and USO place some constraint on its orientation, as does the location of the pole to the first plane. Thus the second plane was chosen to have nearly the same strike as the first plane, dipping moderately southward. This results in a thrusting mechanism with some left-lateral strike-slip component along a moderately dipping,

nearly east-west fault plane, consistent with event 5, also located in Gizhiga Bay.

Event 5 (1979-08-19) is located in slightly east of event 4 (Figure 15). Although its magnitude was moderate (Mb = 5.1), this event exhibited rather poor quality body waves; although short period P-waves were observed at several stations, first motion polarities could be determined for only three stations. Depth phases, however, were observed at all three stations and indicate a focal depth of approximately 14 km. The short period first motion data from stations Danmarks Haven (DAG), Albuquerque (ALQ), and Chieng Mai (CHG), combined with first motion data reported in the ISC, none of which showed anomalously high travel time residuals, were insufficient to constrain the fault geometry of this earthquake. Reports of first motions were confined mostly to European and Soviet stations, covering only the northwest quadrant of the focal sphere.

Fortunately, event 5 exhibited a fair amount of energy on long period surface waves. Using fourteen stations, the resultant Rayleigh wave amplitude radiation pattern (Figure 16) clearly indicates three lobes (the fourth is absent because of lack of recording stations in the southeast quadrant). The lobe in the northwest quadrant is attributed to the station



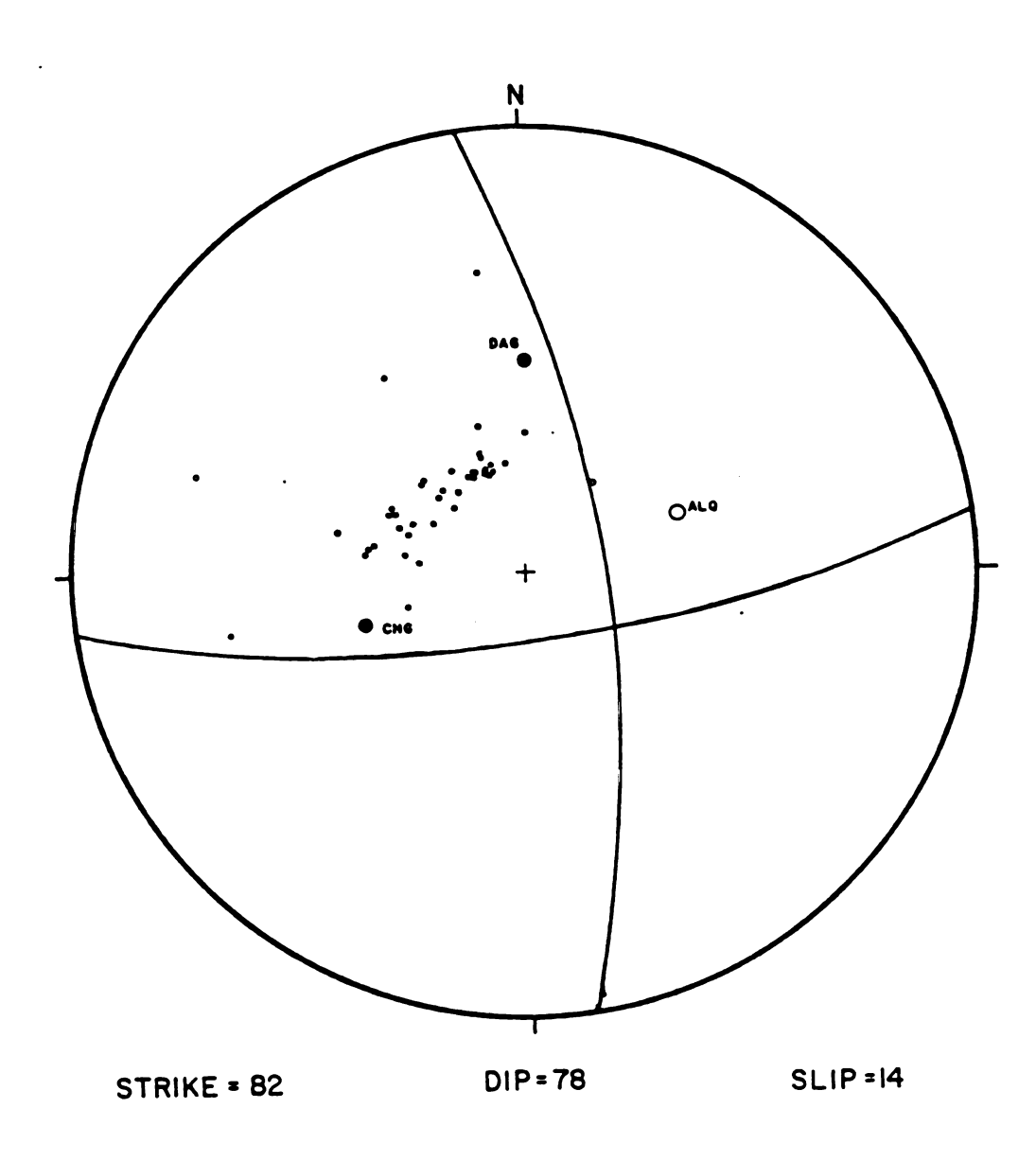


Figure 15: P-wave focal mechanism fro the event of 1979-08-19.

Symbol conventions used are identical to those in Figure 7.

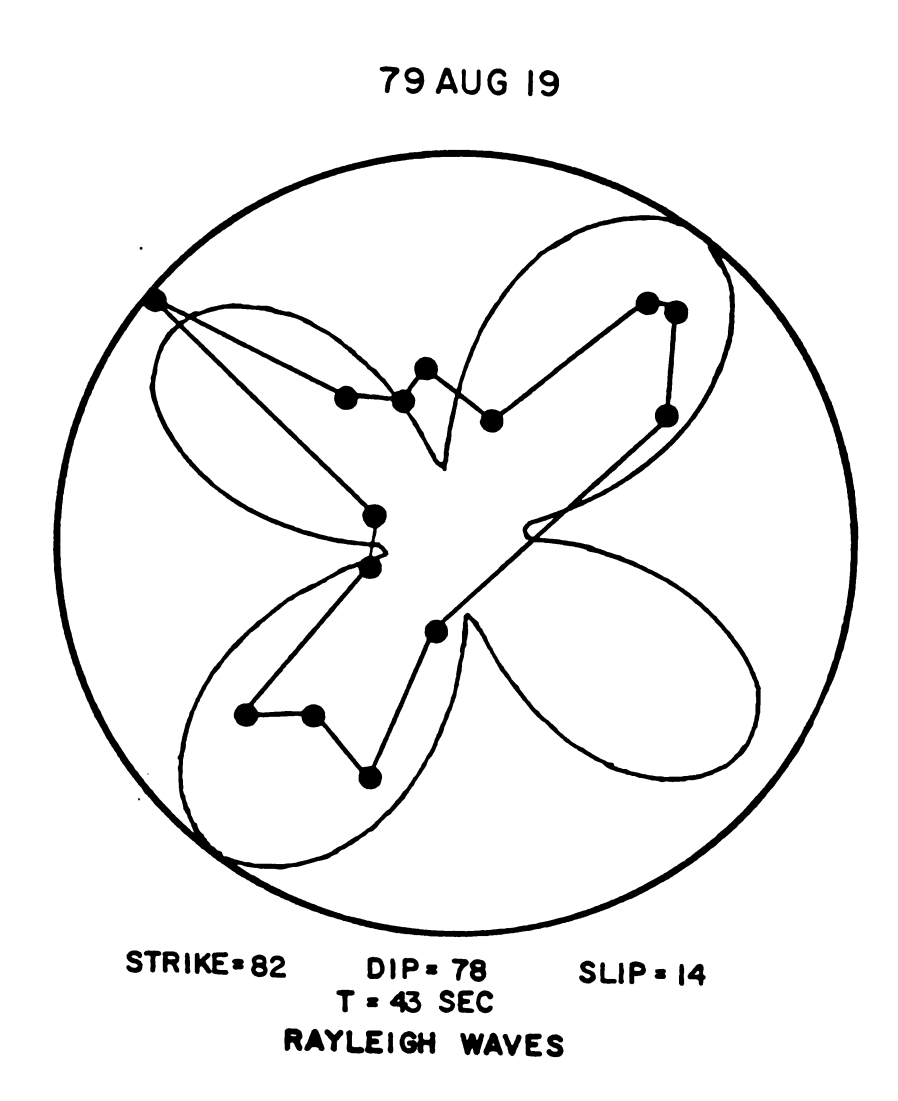


Figure 16: Rayleigh wave amplitude radiation pattern for the event of 1979-08-19. Solid circles represent data points; curved lines represent theoretical Rayleigh pattern generated for this particular fault geometry.

Windhook (WIN); spectral amplitudes for WIN appear to be of fairly good quality so that there is no basis for omitting WIN from the data set. The Rayleigh wave pattern for this event is thus considered acceptable.

Combination of the long-period surface wave and first motion data yield a focal mechanism solution with nearly vertical nodal planes striking north-south and east-west. Because the east-west nodal plane is oriented parallel to the lineation of epicenters in this region, the east-west trending nodal plane is chosen as the fault plane. The resultant mechanism is a left-lateral strike-slip event with a minor thrust component. Koz'min (1984) has also studied this event and obtained a left-lateral strike-slip solution with steeply dipping nodal planes oriented northeast-southwest. Relying heavily upon the orientation of the Rayleigh wave radiation pattern lobes generated for this event, however, the mechanism obtained in this study is preferred.

The moment obtained in this study for event 5 is approximately 2.3 x 10**24 dyne-cm.

Event 6 (1978-06-05) lies in Shelikov Bay just south of Taygonos

Peninsula. The first motion solution was constructed using short period

P-waves read from six station records combined with first motion

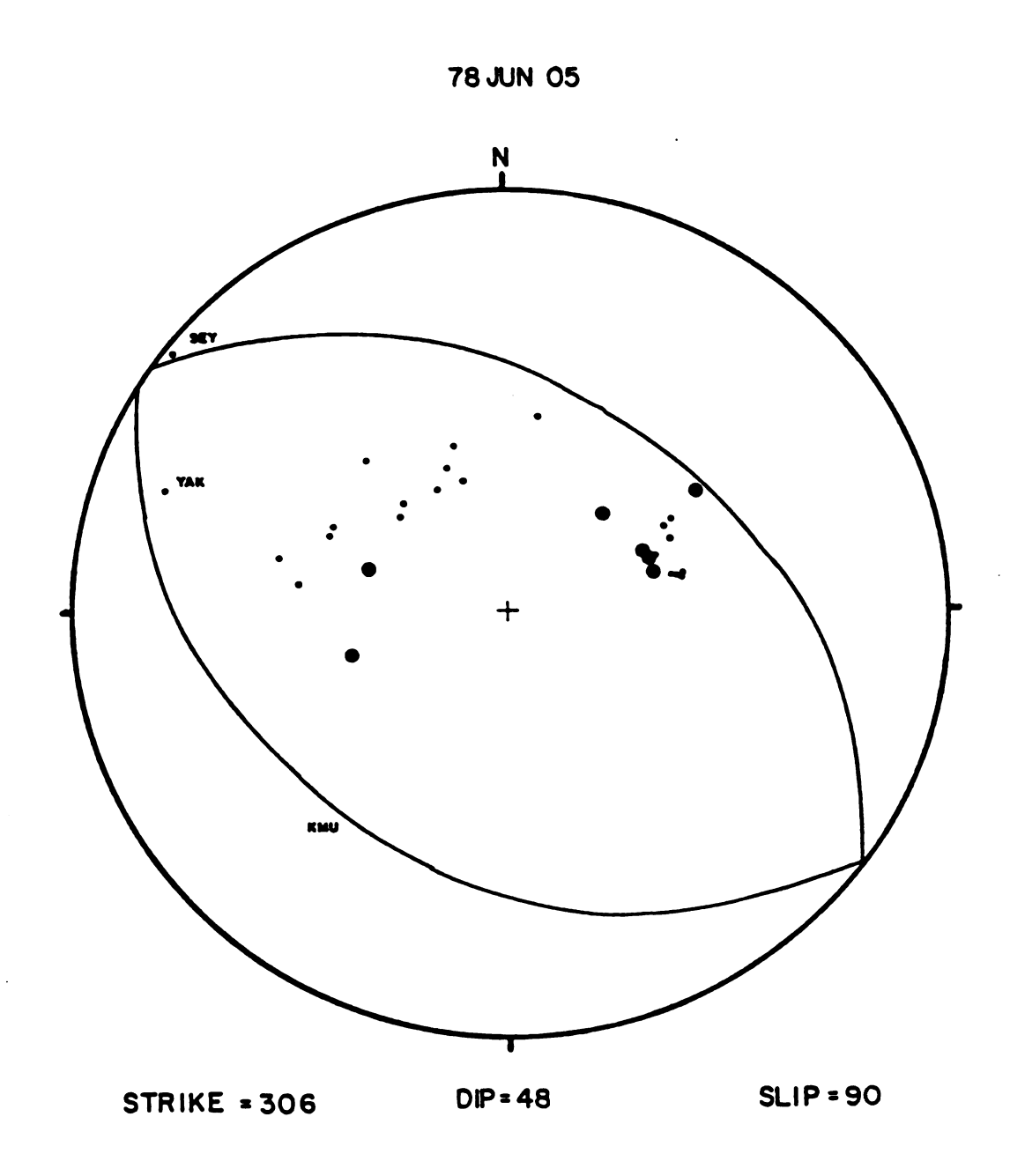


Figure 17: P-wave focal mechanism for the event of 1978-06-05. Symbol conventions are identical to those in Figure 7.

polarities reported in the ISC (Figure 17). Although these data are clearly indicative of a thrust mechanism, the orientation of the two nodal planes is uncertain; most stations recording this event were at considerable teleseismic distances and plotted near the center of the focal sphere.

The reliability of the two Russian stations SEY and YAK and of the Japanese station Kamikineusu (KMU) are critical to this event; travel time residuals for these three stations as calculated by the ISC are 3.5, 5.4, and 13.1 sec, respectively. Hence station SEY is considered reliable, while stations YAK and KMU, which have anomalously high travel time residuals possibly as a result of phase misidentification, are considered unreliable for first motion data. The dilatation reported at SEY unfortunately places almost no constraint on the orientation of nodal planes.

An attempt to establish the fault geometry through the use of Rayleigh wave amplitude radiation patterns proved unsuccessful; relative spectral amplitudes at stations were highly frequency-dependent. The P-wave mechanism alone for this event suggests a pure thrust fault with moderately dipping nodal planes both striking northwest.

Depth phases recorded at five stations for event 6 suggest a focal depth of 10 km, as opposed to the ISC estimate of 56 km.

Koz'min (1984) has studied event 7 (1975-11-04, Mb = 4.8), located at 60.02°N, 160.32°E, in the immediate vicinity of event 6. Using only first motion polarities, he obtained a pure thrust mechanism with moderately dipping nodal planes striking northwest. Koz'min (1984) notes that the strikes of both nodal planes coincide with the strike of faults at the bottom of Shelikov Bay. Ufimtsev (1975) suggests that this transition region is located in the between the Indigirka - Kolyma mountain system and Kamchatka and that the strike of these faults are northwesterly in the region of Shelikov Bay. Thus the structural geology in Shelikov Bay is consistent with a northwest striking fault plane for event 6.

Event 8 (1972-08-03) lies in the northern isthmus of Kamchatka

Peninsula, just northwest of Karaginskiy Island. Although the magnitude

of this event was 5.2, body wave data were of rather poor quality. An

attempt to determine first motion polarities directly from WWSSN records

yielded only four tentative picks; three of these stations which exhibited

little or no energy were designated as lying on or very near nodal planes.

The focal mechanism solution obtained from P-wave data, although not

well constrained, can be interpreted as a strike-slip fault with

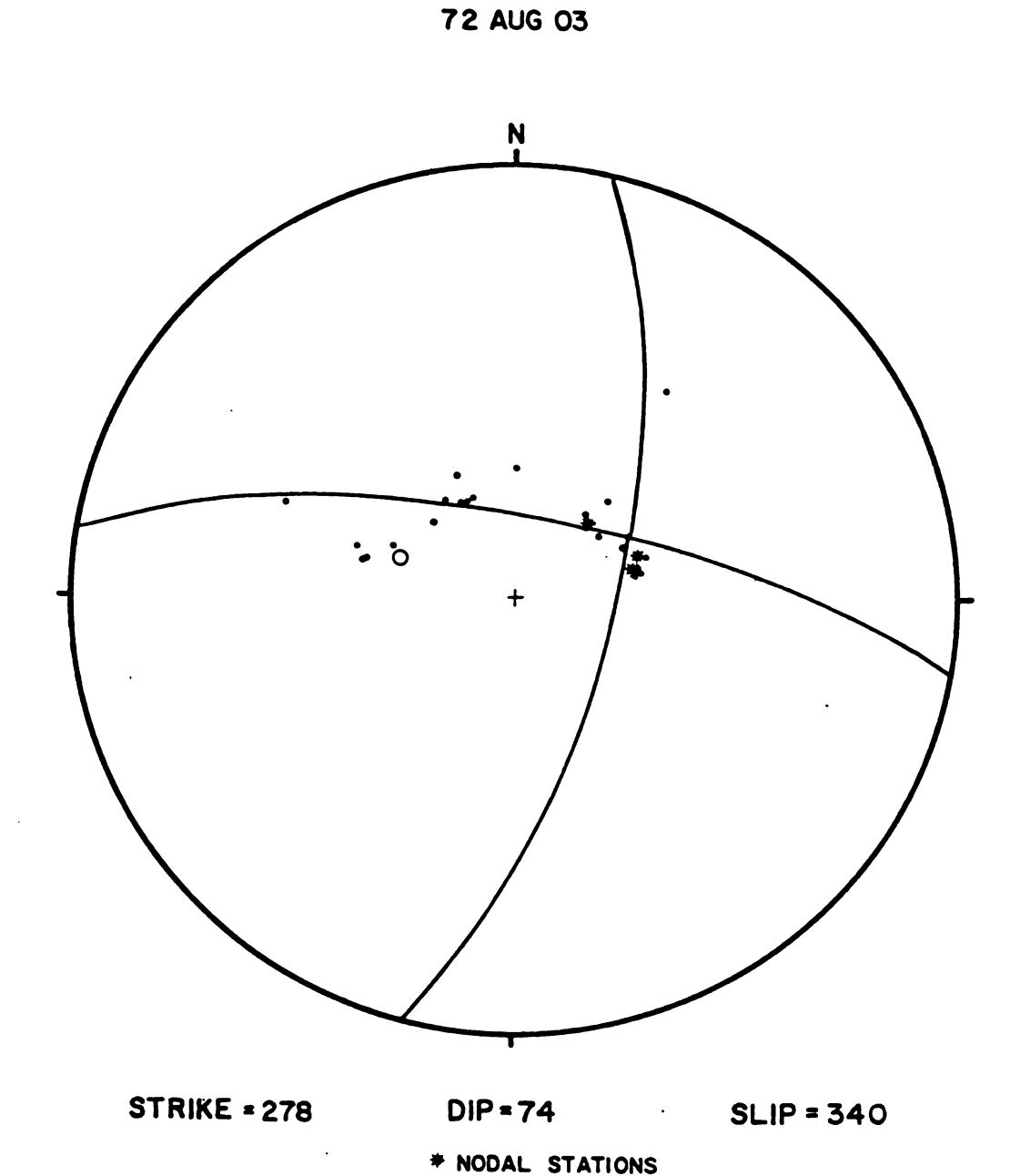


Figure 18: P-wave focal mechanism for the event of 1972-08-03.

Symbol conventions used are identical to those in Figure 7.

72 AUG 03 DIP = 74 **STRIKE = 278** SLIP = 340 T = 43 SEC RAYLEIGH WAVES

Figure 19: Rayleigh wave amplitude radiation pattern for the event of 1972-08-03. Solid circles represent data points; curved lines represent theoretical Rayleigh pattern generated for this particular fault geometry.

steeply-dipping nodal planes striking north-south and east-west (Figure 18). Note that the fault plane solution contains a minor normal faulting component. The proximity of stations located at northeast and east azimuths to the intersection of the nodal planes may account for the large variance of polarities reported at these stations.

An attempt to more precisely constrain the orientation of the nodal planes by body wave modelling proved unsuccessful; synthetic seismograms were extremely sensitive to minor variations in fault geometry, as most stations modelled lay very near the intersection of the two nodal planes (the B axis).

The Rayleigh wave amplitude radiation pattern (Figure 19) generated for event 8 is consistent with the strike-slip fault plane solution obtained from the P-wave mechanism. Spectral amplitudes generated for the fourteen stations used in this Rayleigh pattern were of acceptable quality, so that the radiation pattern is considered reliable.

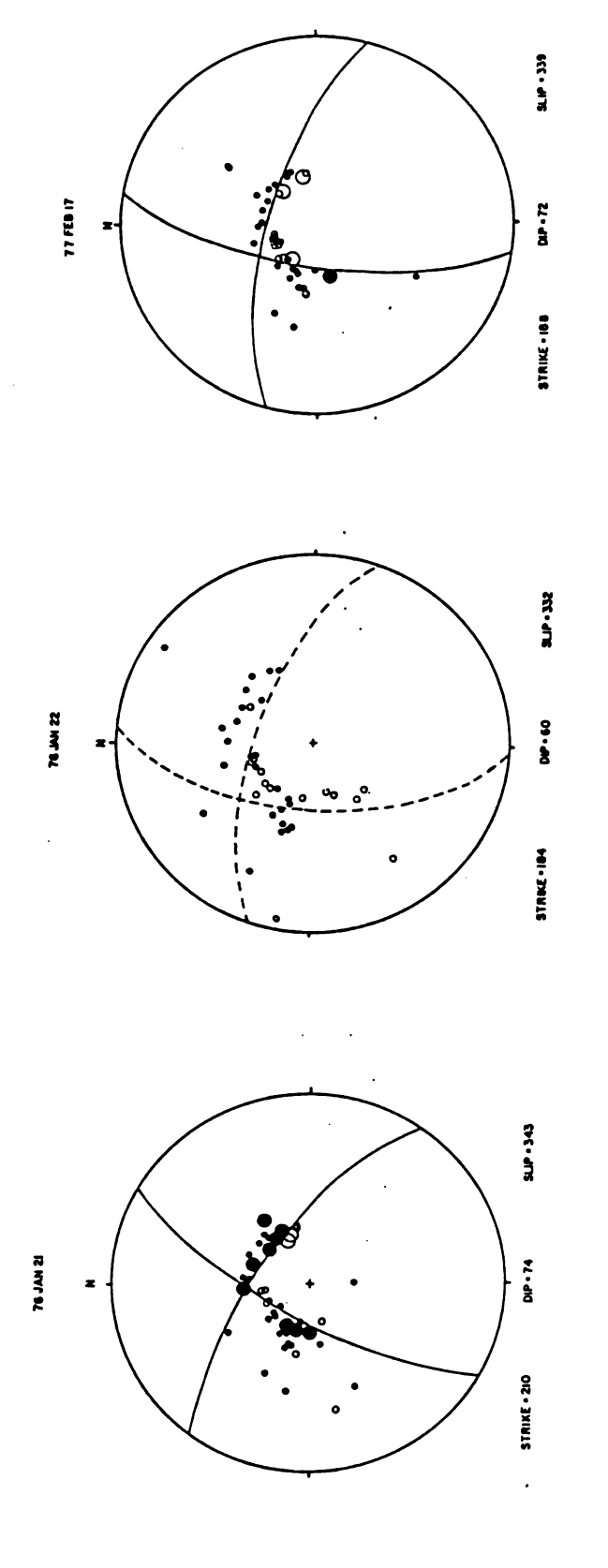
Event 8 is located slightly southeast of event 6 in Shelikov Bay and lies north-northwest of event 9 (1976-01-21) on Karaginskiy Island; the epicenter of event 8 is one which defines the east-west lineation of epicenters trending from the southern Cherskiy Mountains to Karaginskiy

Island. If the north-striking nodal plane is chosen as the fault plane, the resultant mechanism shows right-lateral strike-slip motion paralleling the east coast of Kamchatka, inconsistent with the motion observed for events 3-7 and, as will be seen, inconsistent with events located north of the Kuril-Aleutian arc-arc junction, which are characterized by left-lateral strike-slip or thrusting along a north-striking plane. If the fault plane were chosen as the east-striking nodal plane, displacement would be left-lateral strike-slip along an east-west fault plane, consistent with previous events. For this reason, the east-striking nodal plane for event 8 is designated as the fault plane. Again, P-axes for this event are oriented northeast-southwest.

C. Karaginskiy Island to Kuril-Aleutian Arc-Arc Junction

In January 1976, a sequence of earthquakes, including four teleseismic events ranging in magnitude from 4.2 – 5.4, occurred on Karaginskiy Island, the northern limit of the seismically active band extending from the Kuril-Aleutian arc-arc junction. These earthquake epicenters are confined to a nearly north-south striking zone along the southwest and central parts of Karaginskiy Island (Fedotov et al., 1980). Fedotov et al. (1980) cite a reference that this zone is also the location of a deep Oligocene fault trending along the axis of eastern Kamchatka.

Focal mechanism solutions derived from first motion polarities (read directly from station records and obtained from the ISC) for the two largest events (event 9, 76-01-21, Mb=5.4; event 10, 76-01-22, Mb=5.2) of the sequence are quite similar, exhibiting north-south and east-west striking, moderately steeply dipping nodal planes. Additionally, on February 17, 1977 (event 11) at this same location there occurred an earthquake of magnitude 5.1 whose P-wave solution is nearly identical to those of January 1976 (Figure 20). All three mechanisms may be interpreted as strike-slip motion with a minor component of normal



P-wave focal mechanisms for the Karaginskiy Island sequence illustrating their similar solutions. Symbol conventions used are identical to those in Figure 7. Figure 20:

faulting.

Koz'min (1984) has also studied event 9 (the largest event of the sequence) using only first motion polarities and derived a thrust mechanism with moderately-dipping nodal planes striking west-northwest. For his solution, the nearly east-west striking, southward dipping nodal plane is designated as the fault plane. This fault geometry thus exhibits some left-lateral strike-slip component; displacement is along a plane perpendicular to the strike of the eastern coast of Kamchatka. Savostin et al. (1983) have studied event 9 using only P-wave data and have obtained a pure normal fault striking nearly east-west.

The mechanism obtained for event 9 in this study is preferred over that obtained by Koz'min (1984) and Savostin et al. (1983) for a number of reasons. P-wave polarities read directly from records for several stations for three events occuring on Karaginskiy Island show a consistent clustering of dilatations near the center of the focal sphere, which contradicts the focal solution for a thrust mechanism. Rayleigh wave amplitude radiation patterns generated for the largest event (1976-01-21), although inconsistent with the P-wave focal mechanism solution, show a node striking north-south (Figure 21). Relocation of the

76 JAN 21

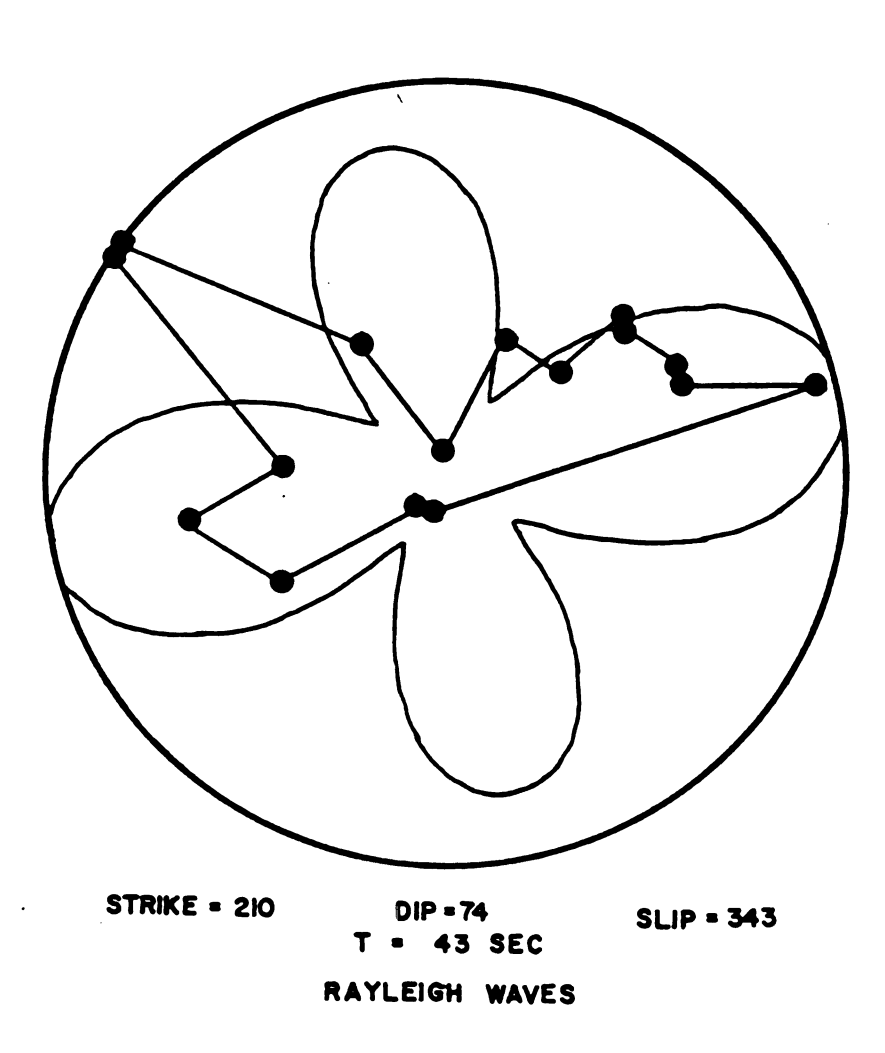


Figure 21: Rayleigh wave amplitude radiation pattern for the event of 1976-01-21. Solid circles represent data points; curved lines represent theoretical Rayleigh pattern generated for this particular fault geometry.

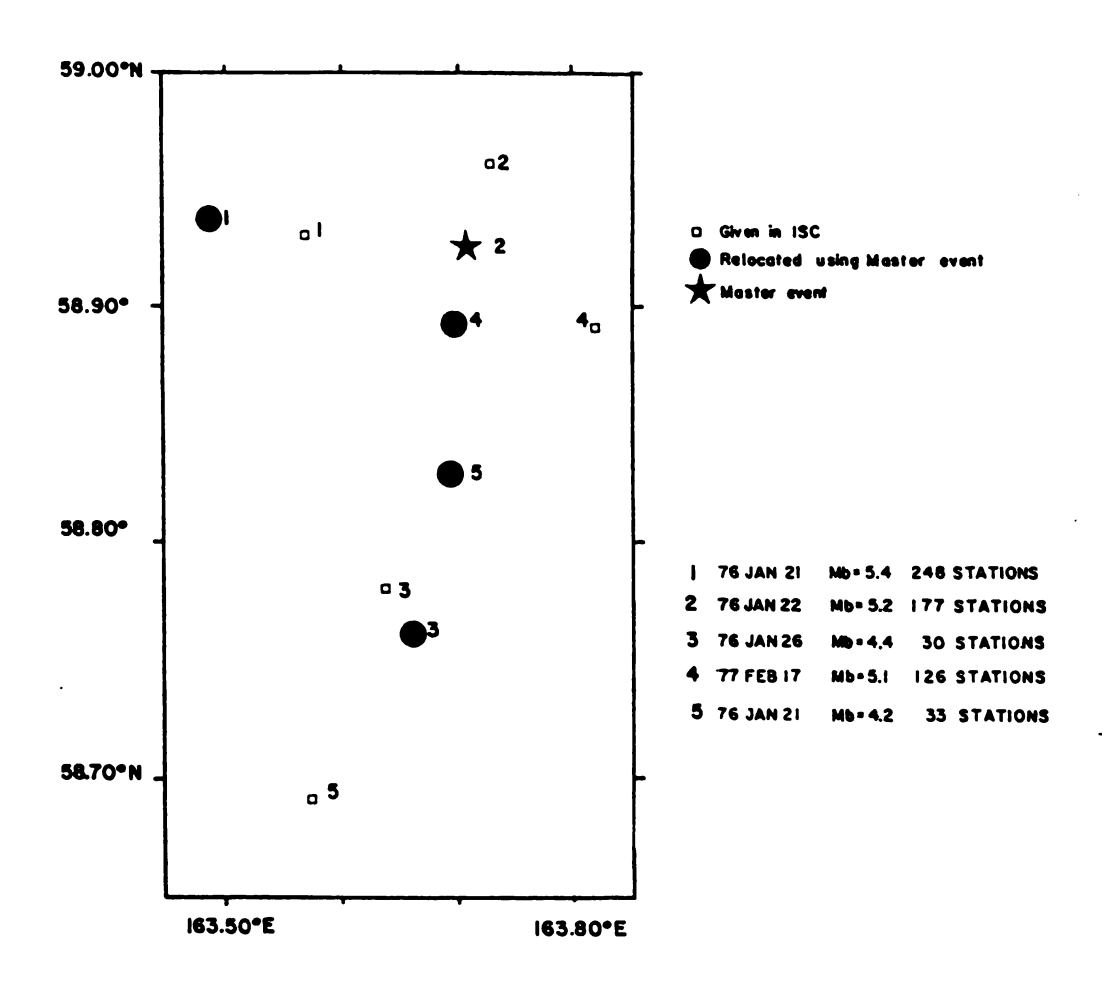


Figure 22: Relocation of aftershocks of the Karaginskiy Island sequence

aftershock sequence for this series of earthquakes, using the event of 1976-01-22 as the master event, show a north-south alignment of epicenters (Figure 22), as does the unrelocated aftershock sequence given by Fedotov et al. (1980) Note that the event of 1977-02-17 also aligns north-south with the sequence of January 1976.

If the north-striking nodal plane is in fact the fault plane, then this earthquake exhibits left-lateral strike-slip motion along a north-south fault plane, similar to events which lie between Karaginskiy Island and the Kuril-Aleutian arc-arc junction. This solution also implies some component of normal faulting. Conversely, if the northwest-striking nodal plane is chosen as the fault plane, displacement would result in right-lateral strike-slip perpendicular to the eastern coast of Kamchatka. The north – south alignment of aftershock epicenters nearly parallel to the east coast of Kamchatka support the choice of the north-striking plane as the fault plane.

For this study, several historical shallow-focus earthquakes previously located in the Bering Sea have been relocated and appear to lie along a shallow seismic belt which can be traced from the Kuril-Aleutian arc-arc junction northward to Karaginskiy Island. Results of these relocations are presented in table 2.

Table 2: Epicenters relocated for this study

DATE	HR-MN-SEC	LAT		MAG(Mb)	DEPTH(km)	LONG MAG(Mb) DEPTH(km) STATIONS	RESIDUAL*
1952-11-30	952-11-30 18-32-23.0 56.41N	56.41N	163.15E	5.0	10	18	1.47
1969-11-23	19-40-00.0	57.80N	162.97E	4.5	10	11	0.76
1969-11-25	10-41-29.0	57.07N	162.60E	4.4	23	6	0.34
1943-03-07	03-01-40.0	59.11N	165.65E	6.7	20	77	2.10
1942-06-10	01-08-05.0	56.92N	164.37E	!	46	21	1.43
1956-01-13		57.16N	163.48E	6.1	33	38	0.79
1945-04-15		57.23N	163.90E	7.0	20	71	1.71
1945-04-15		57.13N	164.01E	6.4	20	20	1.22
1951-01-07	18-31-00.0	53.76N	161.07E	5.2	10	18	0.87

* RMS RESIDUAL IN SECONDS

The majority of fault plane solutions determined for events lying between Karaginskiy Island and the Kuril-Aleutian arc-arc junction have been determined by previous authors (Stauder and Mualchin, 1976; Udias and Stauder, 1964; Cormier, 1975; and Newberry, 1983). Table 3 lists earthquake parameters for these events. Focal mechanism solutions for earthquakes along this trend (Figure 23) indicate that the eastern margin of Kamchatka continues to be subject to compression as far north as 58°N (Cormier, 1975).

Event 12 (1969-11-22) is one of the largest recent earthquakes recorded between Karaginskiy Island and the Kuril-Aleutian arc-arc junction, with a magnitude of 6.3. This event is well-studied (i.e., Zobin and Simbireva, 1977; Cormier, 1975; Stauder and Mualchin, 1976; and Veith, 1974). This event is clearly a thrust fault with north-striking nodal planes. Cormier chooses the steeply-dipping plane as the fault plane; motion is thus high-angle reverse faulting along a north-striking plane.

Zobin and Simbireva (1977) have obtained a mechanism for event 13 (1970-06-19) using P- and S-wave polarities recorded at seismic stations of Kamchatka as well as data published in the Operational Seismological Bulletin of the Institute of the Physics of the Earth, USSR.

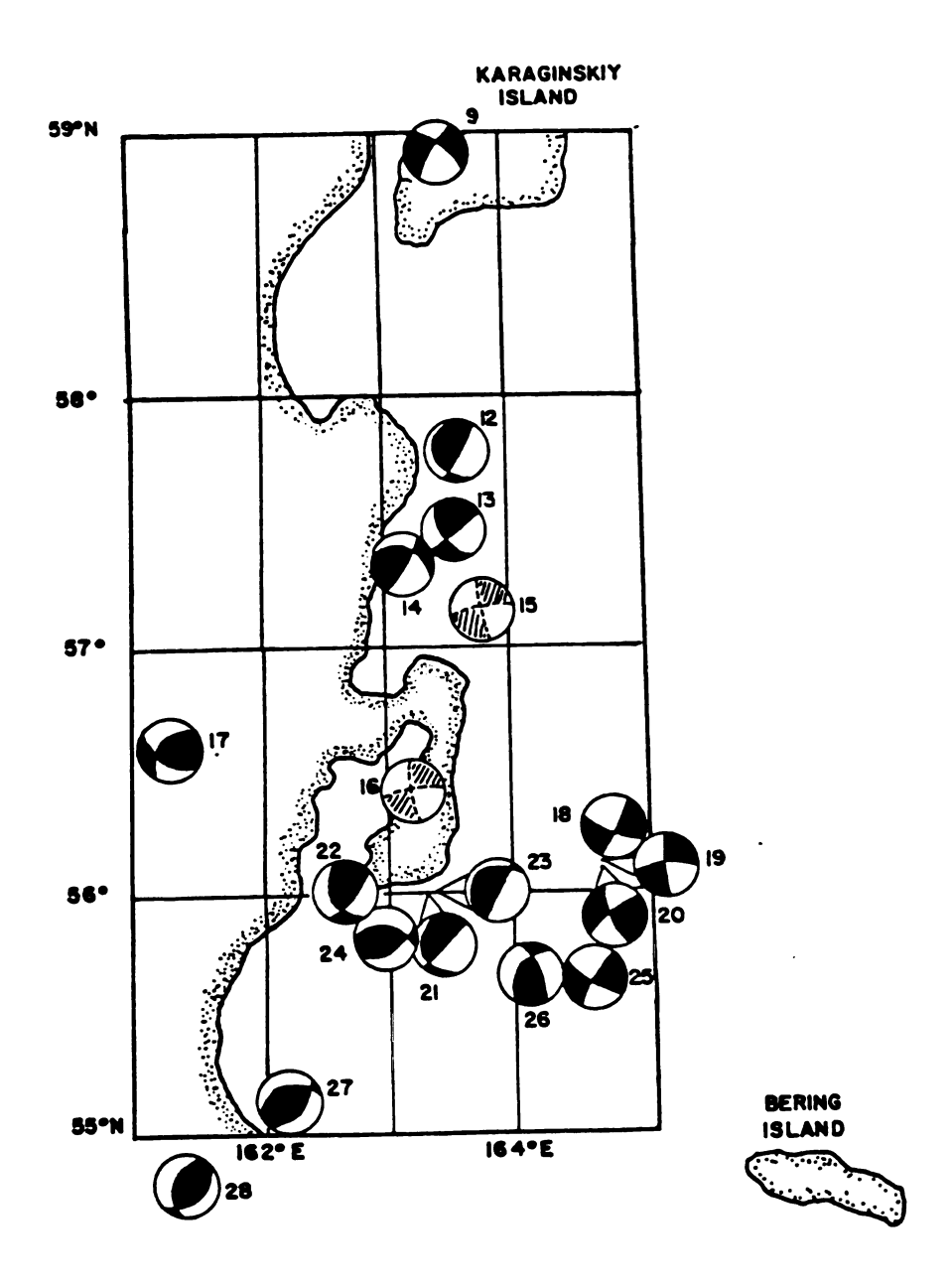


Figure 23: Focal mechanisms of events located between
Karaginskiy Island and the Kuril - Aleutian arc-arc
junction. Compressional quadrants of the mechanisms
are shaded.

Table 3: Kamchatka earthquake mechanisms

EVENT	DATE	LAT	LONG	DEPTH(km)	MAG(Mb)	STRIKE	DIP	SLIP	STUDIES
9 197	6-01-21	58.92N	163.55E	7	5.4	210	74	343	1,6,8
12 196	9-11-22	57.80N	163.50E	33	6.3	178	19	36	2,3,5,13
13 197	0-06-19	57.45N	163.50E	10	5.2	124	76	0	2
14 196	9-12-23	57.32N	163.10E	33	5.4	33	82	49	1,2,3,13
15 194	5-04-15	57.17N	163.71E	: 0	6.8	356	86	5	1,7
16 195	2-11-30	56.41N	163.15E	. 0	7.3	176	84	10	1
17 196	4-11-11	56.58N	163.24E	48	5.5	214	72	31	1
18 196	6-07-19	56.24N	164.83E	20	5.3	120	86	9	3
19 196	5-10-16	56.07N	164.68E	4	5.2	183	73	18	14
20 197	5-01-28	56.60N	164.66E	7	5.1	17	28	7	14
	1-12-15	56.00N	163.26E	•	7.3	149	18	10	3
	9-12-27	56.00N	162.50E		7.0	150	43	44	15
23 197	1-12-15	56.00N	163.30E		6.1	30	80	90	5
	9-01-26	55.84N	162.93E	-	5.5	268	46	107	3
	7-04-12	55.64N	164.59E		5.0	303	90	10	14
	9-11-09	55.61N	164.08	_	5.7	332	61	47	14
	5-04-28	55.10N	162.06E		5.9	256	42	118	3
	0-10-13	54.80N	161.20		6.7	198	54	78	15

ALL EPICENTRAL LOCATIONS FROM ISC

STUDIES (mechanism used is first listed)

- 1. THIS STUDY
 2. ZOBIN AND SIMBIREVA, 1977
- 2. ZOBIN AND SIMBIREVA, 1977
 3. CORMIER, 1975
 5. STAUDER AND MUALCHIN, 1976
 6. SAVOSTIN ET AL., 1983
 7. AVER'YANOVA, 1973
 8. KOZ'MIN, 1973
 13. VEITH, 1974
 14. NEWBERRY, 1983
 15. UDIAS AND STAUDER, 1964

The mechanism obtained by Zobin and Simbireva (1977) shows steeply-dipping nodal planes striking northeast and northwest. The fault plane has been designated by these authors as the northeast-striking nodal plane, resulting in right-lateral strike-slip motion with a minor thrust component. No evidence is presented by Zobin and Simbiereva (1977) to prefer the northeast-striking rather than the northwest-striking plane as the fault plane. If the northwest - striking plane is indeed the fault plane, then displacement becomes pure left-lateral strike-slip nearly parallel to the eastern coast of Kamchatka.

Event 14 (1969–12–23) was studied by Cormier (1975) using both first motions and S-wave polarizations. Cormier (1975) remarks that most P readings were compressional, and the S-wave polarization pattern indicates a nearly horizontal axis of compression; the orientation of nodal planes are thus not well-constrained. His solution indicates a thrust fault along nearly east-west planes, having a minor strike-slip component. Another solution for event 14 was obtained in this study through the use of short-period first motion data read from station records and reported in the ISC. The east-west nodal plane is unconstrained and was chosen to have the same orientation as that obtained by Cormier (1975).



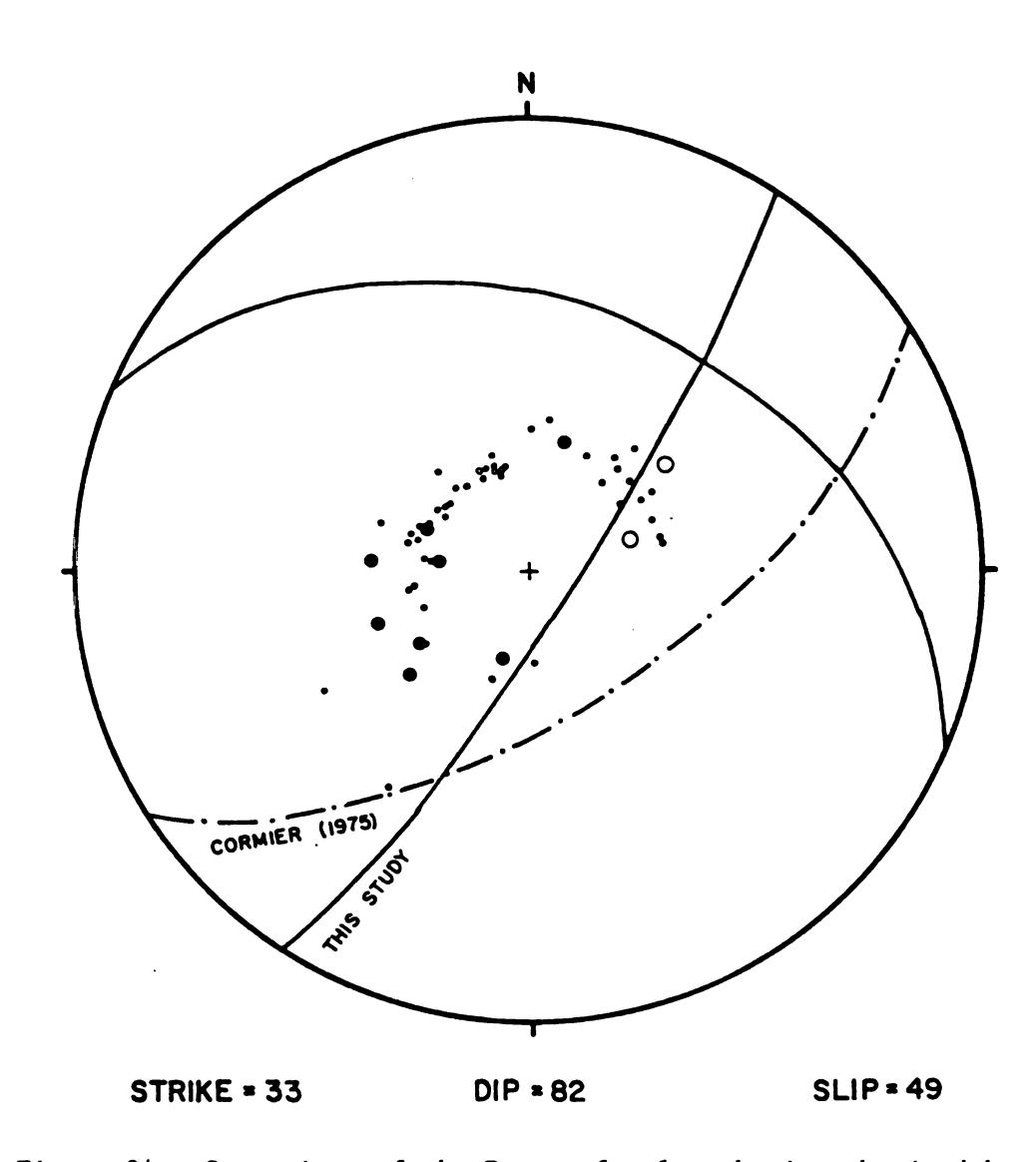
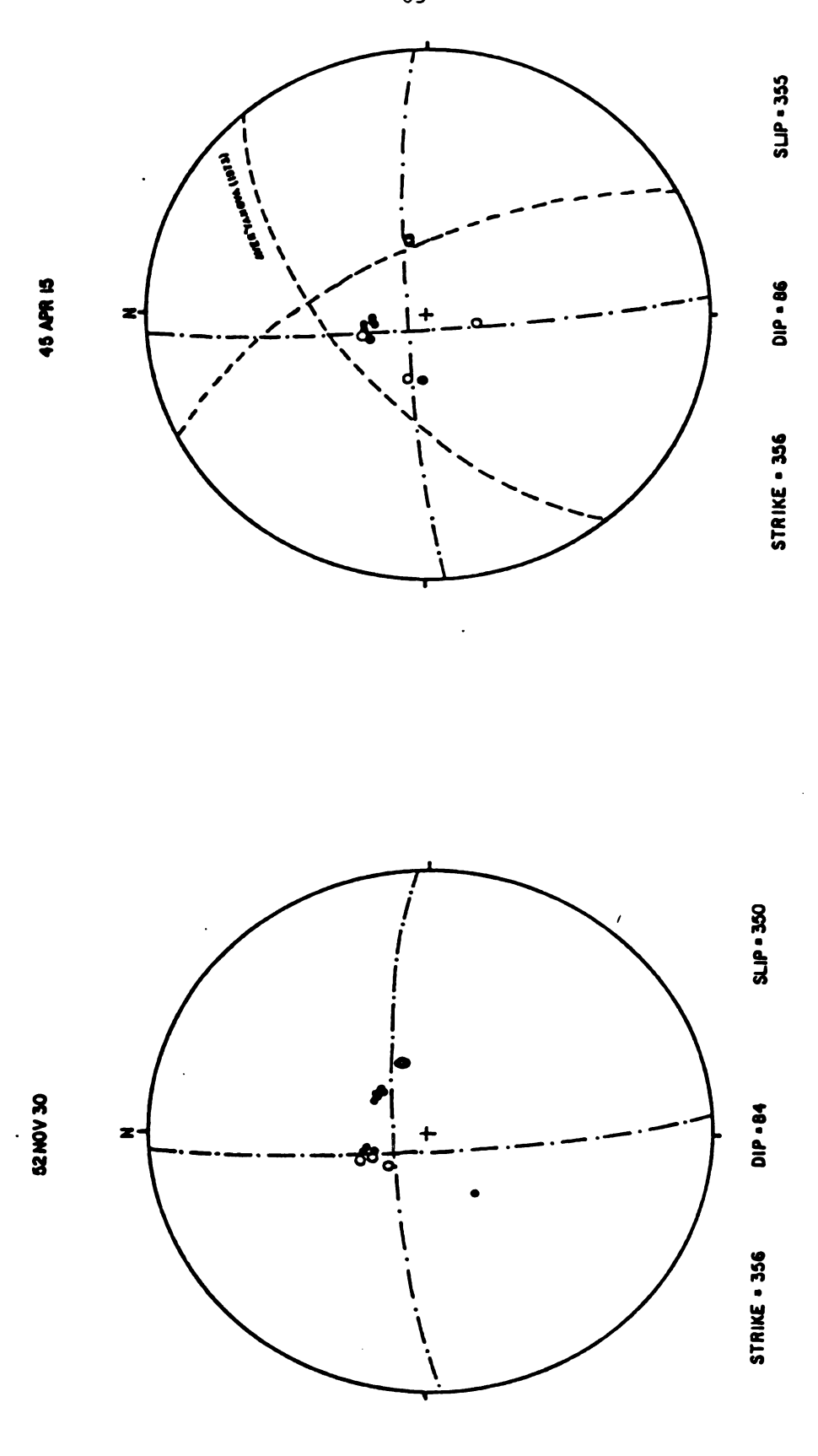


Figure 24: Comparison of the P-wave focal mechanism obtained by Cormier (1975) and in this study for the event of 1969-12-23. Symbol conventions used are identical to those in Figure 7.

The two dilatations near the center of the focal sphere in the northeast quadrant make it possible to rotate the northeast-striking nodal plane northward and increase the dip angle of this plane to include the dilatations within the southeast quadrant (Figure 24). The resultant mechanism is still a thrust fault, but exhibits more of a strike-slip component.

Events 15 (1945-04-15) and 16 (1952-11-30) (Figure 25) are historic events; the only available data for these events were first motion polarities reported in the ISS. Although the number of first motions are limited (12 for event 15 and 16 for event 16), their azimuthal distribution within the focal sphere are not inconsistent with strike-slip mechanisms with north-south and east-west striking nodal planes. Note that these pure strike-slip mechanisms are inconsistent with all other mechanisms in figure 23, which have a considerable thrust component. For this reason, these two poorly-constrained fault plane solutions may not be considered reliable.

Aver'yanova (1973) also studied the event 15 using only P-wave data and obtained a thrust mechanism with a considerable strike-slip component. Nodal planes for her solution strike northeast- southwest and



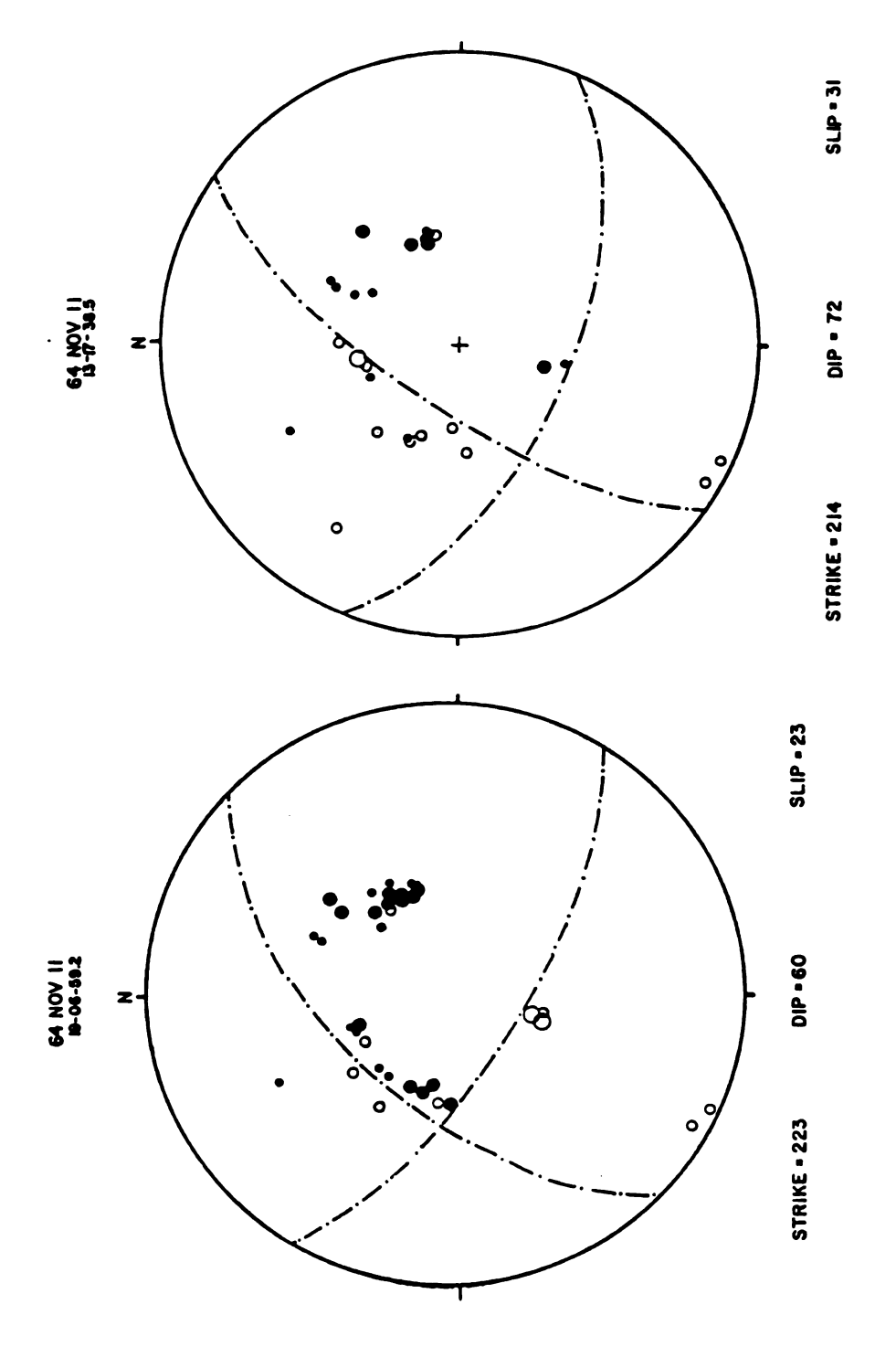
Symbol conventions used P-wave mechanisms for historic events of northeastern Kamchatka. are identical to those in Figure 7. Figure 25:

are oriented 45° from the nodal planes of the solution obtained in this study. It is quite possible that Aver'yanova used a different velocity model for these mechanisms, which influences the take-off angles and thus results in a different focal sphere projection of the station (Appendix A).

If the north-south nodal plane is chosen as the fault plane for events 15 and 16, the resulting mechanism shows left-lateral strike-slip motion along a fault plane which parallels the east coast of Kamchatka, similar to solutions obtained for event 13 and to the Karaginskiy Island sequence.

Prinicipal stress axes for all of these events are consistently oriented in a northeast-southwest direction.

Events 17a and 17b (1964–11–11) (origin times are 13:17:38.5 and 19:06:59.2, respectively) are the largest in a series of approximately 30 earthquakes which occurred within eastern Kamchatka northwest of the Kuril-Aleutian arc-arc junction (Figure 26). The second largest event in the series occurred six hours prior to the largest event in the same location. First motion data indicate that both events exhibit similar mechanisms: thrust faults with some component of strike-slip motion. These events are located in an area which could allow for faulting along the Central Kamchatka basin and Eastern Ranges.



P-wave mechanisms for the events of 1964-11-11 showing their similar solutions. Symbol conventions used are identical to those in Figure 7. Figure 26:

Several events located slightly north of the Kuril-Aleutian arc-arc junction have been studied by previous authors (Stauder and Mualchin, 1976; Cormier, 1975; Newberry, 1983; and Udias and Stauder, 1964) and are illustrated in figure 23. These events are all characterized by a considerable amount of thrust with some strike-slip component. The large variance of principle stress axes orientations for events in this region may be related to slab contortion and/or interaction at the Kuril-Aleutian arc-arc junction.

The seismicity west of Bering Island is aligned roughly north-south along a northward-trending trough in the area (Newberry, 1983). Fault plane solutions obtained in the far western Aleutians by Newberry (1983) may imply some northward movement of the western Aleutian ridge with respect to Kamchatka Peninsula along the strike-slip zone extending northward from Bering Island. Events just south of the Kuril-Aleutian arc-arc junction along the east coast of Kamchatka are characterized by a northwest-dipping fault plane consistent with underthrusting of the Pacific plate beneath Kamchatka Peninsula.

DISCUSSION OF RESULTS

Figure 27 is a summary of focal mechanisms obtained in this study combined with those determined by previous authors. Events in the southern Cherskiy Mountains are dominated by left-lateral strike-slip faults along a northwest plane. These strike-slip faults trend across, but are not traced beyond, the depressions. The region extending from Shelikov Bay to Karaginskiy Island is characterized by thrusting and left-lateral strike-slip events with some component of thrust. The westward extension of this lineation coincides with the southernmost event of the southern Cherskiy Mountains. Events of the seismic zone extending from Karaginskiy Island to the Kuril-Aleutian arc-arc junction are dominated by thrusting along a north-south plane with oblique strike-slip.

The three-plate configuration of the Eurasian, North American, an Pacific plates chosen by Chapman and Solomon (1976) (Figure 28, model C) extends the Eurasia-North America plate boundary along the Sea of Okhotsk through the islands of Sakhalin and Hokkaido; the Sea of Okhotsk is thus attributed to the North American plate. However, Chapman and

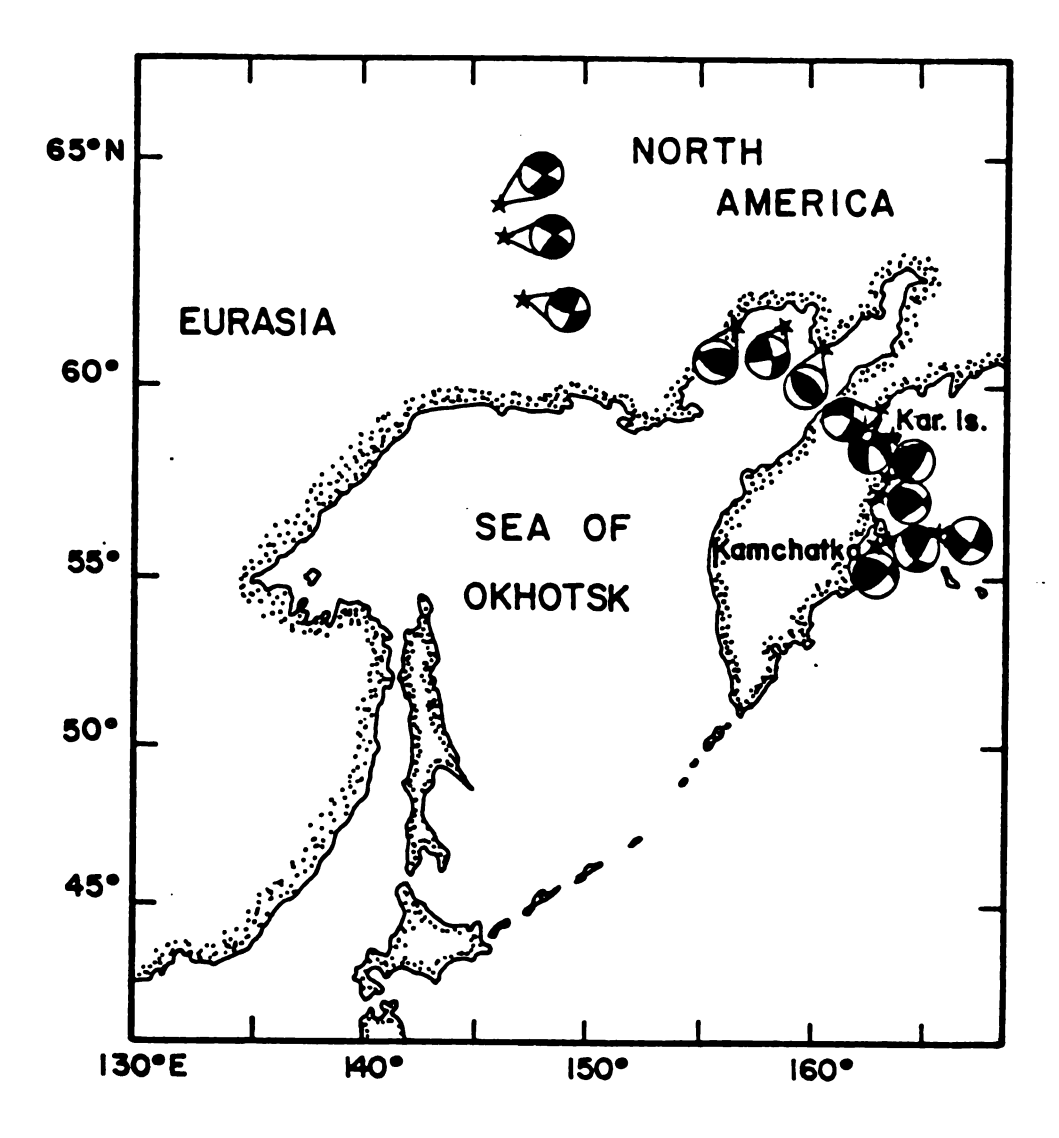


Figure 27: Summary of focal mechanisms along the northeastern Sea of Okhotsk. Compressional quadrants of the mechanisms are shaded.

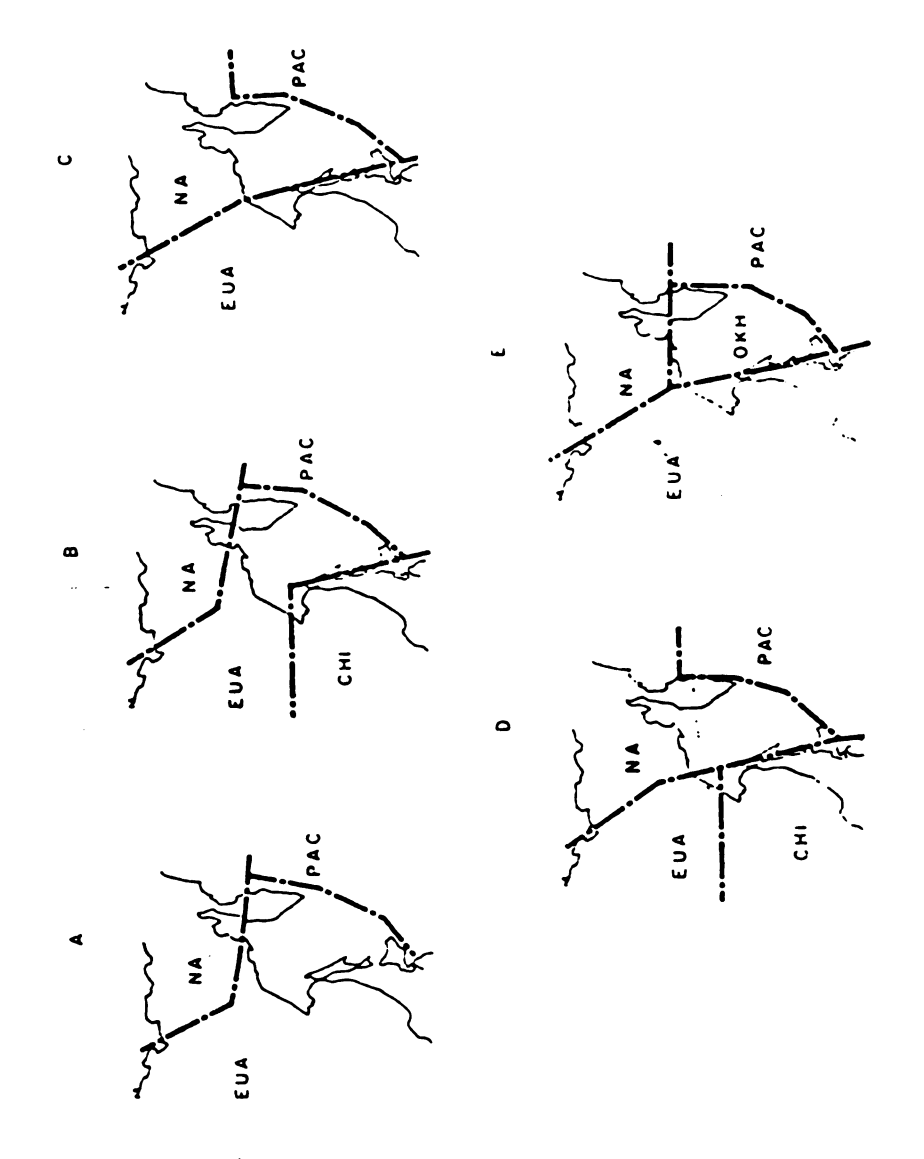


Figure 28: Proposed plate configurations for the Eurasia and North America plates (from Chapman and Solomon, 1976)

Solomon (1976) noted that if events 1 and 3 are interpreted as left-lateral faults occurring on a single plate boundary, the two slip vectors uniquely define a pole of rotation at 65°N, 148°E, clearly distinct from the Eurasian-North American pole of Minster and Jordan (1978) and of Chapman and Solomon (1976) for this plate configuration. Therefore, the three earthquakes in the southern Cherskiy Mountains do not lie along the Eurasian-North American plate boundary proposed by Chapman and Solomon (1976); these earthquakes possibly define another plate boundary.

Another plate configuration to be considered of the Eurasian, North American, and Pacific plates in northeast Siberia delineates the boundary between these two plates through the southern Cherskiy Mountains, north of Magadan, through Shelikov Bay, to Karaginskiy Island, then southward to the Kuril-Aleutian arc-arc junction (Figure 28, model A). The Sea of Okhotsk is thus attributed to the Eurasian plate for this model.

The northern coast of the Sea of Okhotsk is the site of a late Mesozoic suture zone, whereas the region north of the Kuril-Aleutain arc-arc junction was the locus of westward directed subduction during late Miocene or early Pliocene (Fujita, 1979; Scholl et al., 1975). These fossil

subduction zones are most likely zones of weakness along which recent tectonic activity is concentrated. However, the proposed plate boundary, delineated on the basis of seismicity, cuts across the Mesozoic suture zone. Savostin et al. (1983) have described a "Gizhiga-Karaginskiy extension zone" which extends from Gizhiga Bay to Karaginskiy Island, discordantly crossing topographic features without significant surface manifestations. However, there is no evidence presented in their paper to indicate such a structure, nor were any seismic reflection or refraction data available in this region to assess the validity of their interpretation.

Admittedly, the structural features along the northeastern Sea of Okhotsk are quite complex and do not indicate the presence of a plate boundary in this region. If the boundary is in relatively early stages of development, however, or if relative motion between the Eurasian and North American plates is slow along the northeastern Sea of Okhotsk (Savostin et al., 1982, suggest a rate of 1-1.5 cm/y) the boundary may manifest itself minimally in topographic features. That the boundary is not a continuous fault but consists of several fault splays (similar to the San Andreas fault) must also be considered.

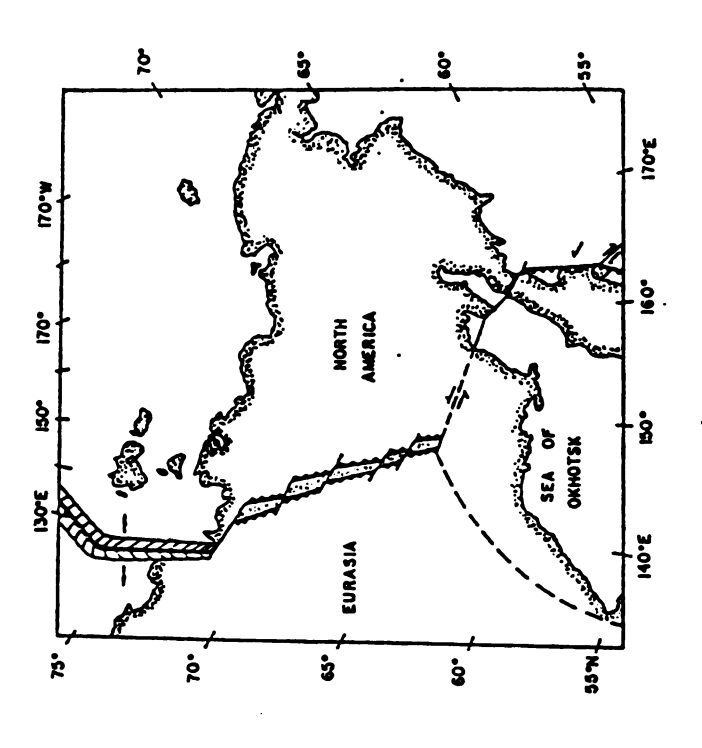
The most convincing evidence for the plate boundary proposed in

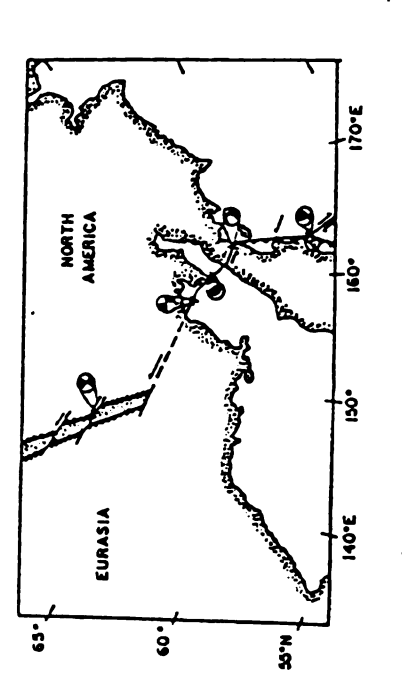
model A lies in the lineation of earthquake epicenters extending from the southern Cherskiy Mountains to the Kuril-Aleutian arc-arc junction.

Figure 29 shows this boundary along with a schematic representation of the tectonics of the northeastern Sea of Okhotsk and representative focal mechanisms.

The strike-slip events in the southern Cherskiy Mountains offset the fault-bounded depressions which most probably separate the Eurasian and North American plates. The events from Shelikov Bay to Karaginskiy Island are proposed to lie along the fault zone which delineates the boundary between the North American plate and the Sea of Okhotsk. The anomalous thrust fault (event 6) may result as offset portions of the boundary resist lateral motion as the Sea of Okhotsk rotates counter-clockwise relative to the North American plate. West-northwest convergence of the North American plate against the northeastern portion of the Sea of Okhotsk may be manifested in the zone of shallow-focus earthquakes extending from Karaginskiy Island to the Kuril-Aleutian arc-arc junction.

Finally, Chapman and Solomon (1976) have proposed a plate configuration which consists of three plates: the Eurasian and North





North American boundary with representative focal mechanisms. Diagram to the right shows plate configuration in northeast Asia with the addition of the Okhotsk plate. Eurasian - North American plate boundary proposed by this study and a new plate configuration for northeast Asia. Diagram to the left illustrates Okhotsk -Figure 29:

American plates and a separate Okhotsk plate (Figure 28, model E). The western boundary of the Okhotsk plate extends though Sakhalin and Hokkaido to the southern Cherskiy Mountains as in model C. The northeastern boundary of the Eurasia-North America plates extends though the southern Cherskiy Mountains, through Shelikov Bay, to the Kuril-Aleutian arc-arc junction. The results of this study indicate that the delineation of the northeastern boundary is quite possible.

Futhermore, results of calculations for poles of rotation (Appendix B) for this study suggest three separate poles of rotation in northeast Siberia, supporting the existence of a separate Okhotsk plate.

TECTONIC IMPLICATIONS

Given this configuration of the Eurasian and North American plates, where does their pole of relative rotation lie? Minster and Jordan (1978) have positioned the pole within northeast Siberia at 65.85°N, 132.44°E, just west of the southern Cherskiy Mountains; they note that this pole does not fit their data south of 60°N. Chapman and Solomon (1976), combining slip vectors for events in Sakhalin, the southern Cherskiy Mountains, and the Arctic, have calculated the Eurasian - North American pole to lie at 61.8°N, 130.0°E, along the northwestern shores of the Sea of Okhotsk. The North American plate rotates clockwise with respect to Eurasian plate. Both of these pole positions predict spreading at the Arctic Mid-Ocean Ridge but do not account for the slip vectors obtained for the strike-slip events in the southern Cherskiy Mountains and Shelikov Bay.

Evidence exists that suggests the Eurasia-North America pole of rotation has recently shifted from the southern northeast Siberia and now lies at a more northerly position (Cook et al., 1984). First of all, the

Balgan-Tas, a volcano of highly alkaline basalt which formed during an extensional period in northeast Siberia (Churkin, 1972) has been inactive since Pliocene - Pleistocene time. Recent focal mechanism solutions obtained by Cook et al. (1984) south of the Lena River delta show no indications of a tensional regime. These events, as well as the three strike slip events in the southern Cherskiy Mountains, exhibit some component of thrusting and closure between the North American plate and the plate west of it. Additionally, recent tectonics of the Cherskiy Mountains and Moma Range indicate uplifts of considerable magnitudes (Savostin and Karasik, 1981; Churkin, 1972; Rezanov and Kotchetkov, 1962). Hence the Moma region in the southern Cherskiy Mountains is not presently the continental continuation of the Arctic Mid-Ocean Ridge, but is now subject to compression.

Finally, the results of calculations for the pole(s) of rotation within northeast Siberia using data from the north Atlantic to Sakhalin and the Kuril-Aleutian arc-arc junction implies that there are three separate poles of rotation in northeast Siberia; the Eurasian-North American (72.15°N, 130.50°E), the North America-Okhotsk (69.00°N, 158.00°E), and the Eurasia-Okhotsk (61.00°N, 130.30°E) (Figure 30). A more detailed

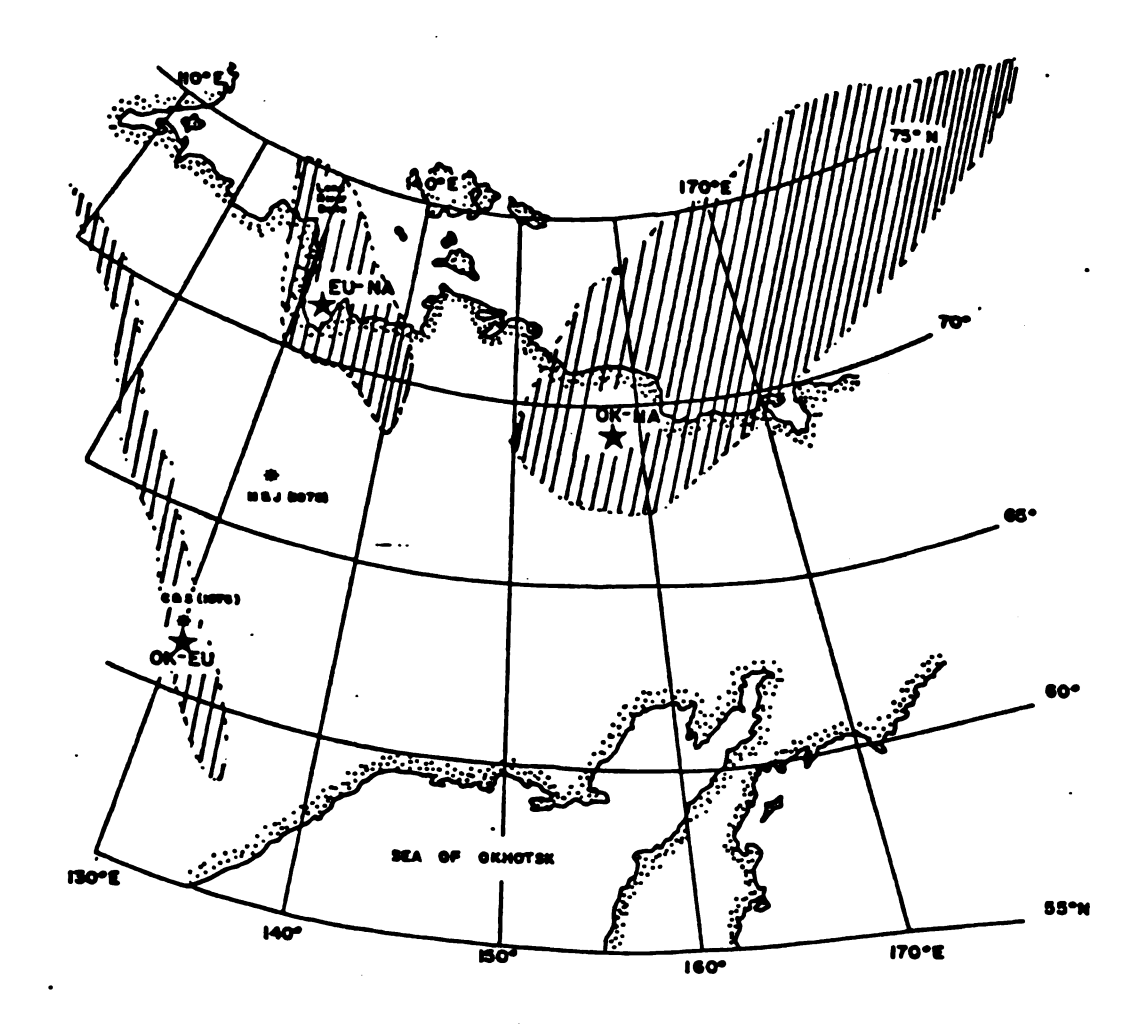


Figure 30: Results of poles of rotation calculations. Eurasian North-American pole obtained by previous authors (M & J:
Minster and Jordan, 1978; C & S: Chapman and Solomon, 1976)
designated by asterisks. Poles obtained in this study
designated by stars. Shaded regions indicate confidence
ellipses for the poles obtained in this study.

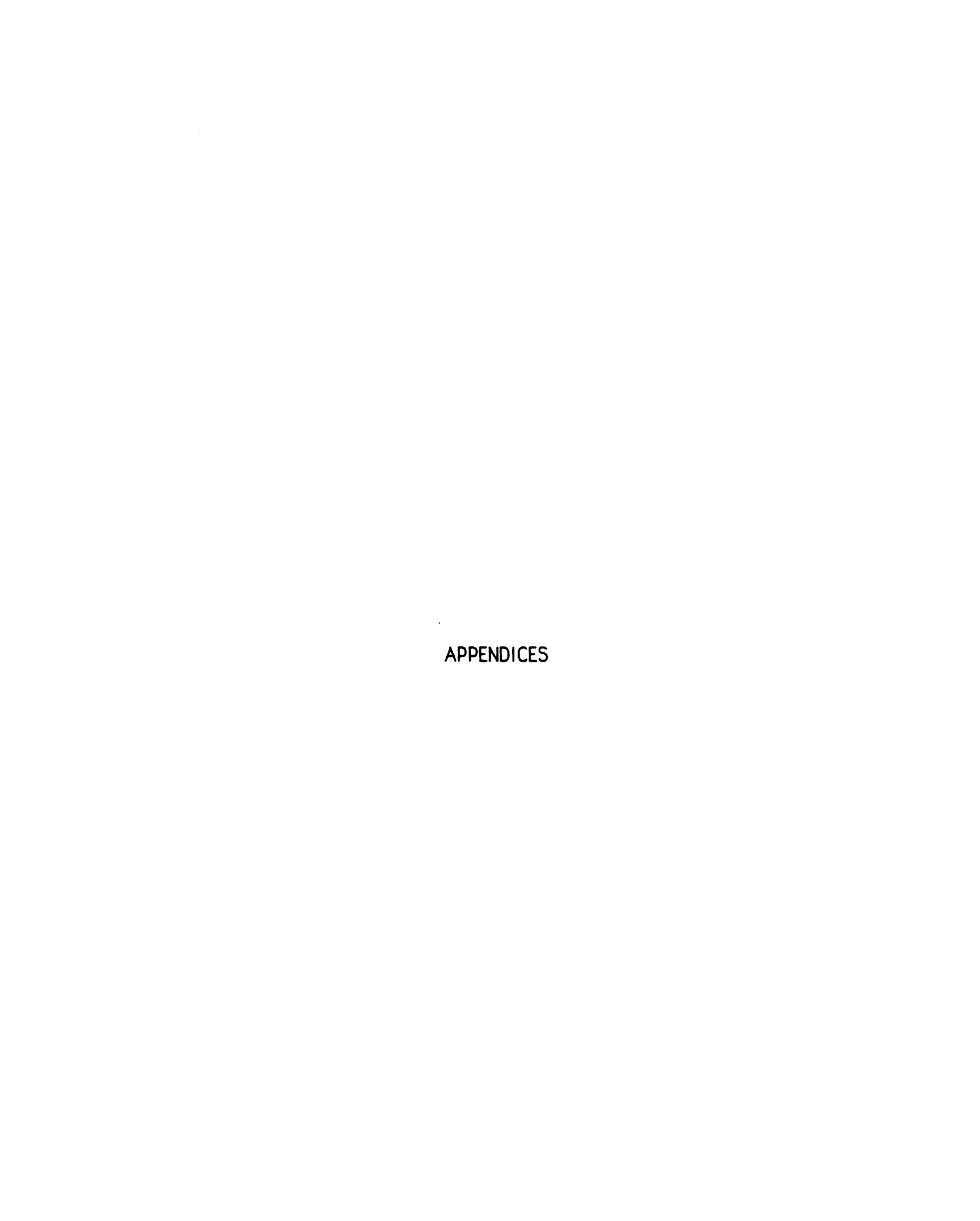
discussion of the pole of rotation calculations and its implications is given in Appendix B.

Spreading in the Arctic Mid-Ocean Ridge, strike-slip events in the southern Cherskiy Mountains, strike-slip and thrusting in Shelikov Bay, and oblique thrusting along the northeast coast of Kamchatka Peninsula are observed. These tectonics are predicted by the pole positions obtained in this study for the Okhotsk plate and adjacent plates and the relative plate motions about these poles.

CONCLUSIONS

Focal mechanism solutions obtained from P-wave and long-period
Rayleigh wave data in the northwestern Sea of Okhotsk region indicate
that the southern Cherskiy Mountains are dominated by left-lateral
strike-slip motion along a northwest-striking fault plane; Shelikov Bay is
dominated by thrusting or thrusting with some component of left-lateral

strike-slip; and the region north of the Kuril-Aleutian arc-arc junction exhibits oblique thrusting with some left-lateral strike-slip displacement. These fault plane solutions and the distribution of seismicity in the northeastern Sea of Okhotsk region suggest the existence of a plate boundary between the North American plate and the Sea of Okhotsk; the Sea of Okhotsk rotates counterclockwise with respect to the North American plate. The results of the pole calculations also imply that there are indeed three separate poles of rotation in northeast Siberia, supporting the existence of a separate Okhotsk plate.



APPENDIX A

DATA ANALYSIS TECHNIQUES

I. Hypocentral Relocations

Epicenters of several historic events located off the eastern coast of Kamchatka Peninsula in the Bering Sea were relocated using a computer program developed by Hiroo Kanamori. Earthquake parameters of focal depth, origin time, latitude, and longitude are calculated using P-wave arrival times recorded at stations at epicentral distances of less than 90 degrees. These observed arrival times are compared to theoretical P-wave arrival times derived from Jeffries and Bullen (1970) travel time tables. These tables are the result of average travel times observed all over the globe; thus the program assumes a spherically symmetric velocity model. Travel-time residuals, the difference between observed and calculated travel times, are then minimized by a least squares method which allows the hypocenter and origin time to vary.

Latitude and longitude of the hypocenter are most often of greater

origin time. Focal depth may thus vary at the expense of the origin time.

Because the travel time tables used in this program assume an average velocity structure, focal depths obtained by this method do not usually agree with observed depth phases or depths obtained by body wave modelling.

The ISC Bulletin initially locates the earthquake epicenter in the following manner. The ISC considers observations whose residuals have an absolute value between 20 and 50 s as being unassociated with the event. Duplicate readings for the same event are eliminated, and larger station weightings are given to those observations received directly from the stations themselves. All observations and epicentral estimates of the ISC are then examined by a seismologist to insure that travel times used in calculations for the event are only those associated with the event. Once the final set of travel times has been obtained, the revised estimate is re-calculated with only those data.

The ISC Bulletin initially "locates" the event, so that "relocating" the hypocenter must involve some technique in order to obtain different results. Perhaps the most effective means of relocating the smaller

earthquakes is to weight stations with high residuals with a value of zero, especially for stations at great (70 - 80 degrees) epicentral distances from the earthquake, since the misidentification of phases is more likely as the signal to noise ratio usually decreases as a function of distance. Residuals in excess of a few seconds for these stations were thus regarded as anamalous. Travel times observed at smaller epicentral distances were generally allowed a higher residual, since these travel times are largely influenced by local crustal structure. Other methods used in the relocation program included fixing the depth or origin time and allowing only the epicentral parameters to vary. Results of relocations of earthquakes along the northeast coast of Kamchatka Peninsula are presented in table 2 in the text of this paper.

The program also allows for relocation of other events relative to a master event in the near vicinity by assuming that the residuals calculated for the master event are the result of inhomogeneities in the earth between the earthquake and receivers. These residuals are applied as station corrections for the events located near the master event. An attempt to use this master event relocation technique for the three events in Shelikov Bay, using each event as the master event in separate

attempts, proved successful only in varying locations reported in the ISC by more than a few tenths of a degree. Implementation of the master event program did prove successful, however, in realigning the epicenters of the Karaginskiy Island aftershock sequence along a more north-south trend.

II. Focal Mechanism Solutions

The two methods used in this study to obtain earthquake mechanisms were body wave polarities and Rayleigh wave radiation patterns.

The first method utilizes the polarity of P-waves received from the earthquake at various stations. Polarities are then plotted on an equal area projection stereonet as a function of incidence angle of the ray and azimuth of the recording station relative to the earthquake epicenter.

Pho and Behe (1972) have calculated incidence angles which were used in this study for various focal depths and epicentral distances using Herrin

et al. (1968) travel time tables.

The focal mechanism solution is plotted as a lower hemisphere projection, with each point plotted representing the point of emergence of a ray from the focal sphere. The assumed double couple source mechanism requires compressional and dilatational quadrants which are delineated by two orthogonal planes, but does not enable one to distinguish between the fault plane and the auxiliary plane. Methods by which the fault plane may be determined are the distribution of aftershocks relative to the epicenter and consistency of the fault plane orientation with a knowledge of regional structure or tectonics.

Several sources of error are encountered by the method of P-wave polarity. Lack of recording stations within close epicentral distances and poor azimuthal distribution of stations lead to less well constrained orientation of the nodal planes. Additionally, the take-off angle of the ray is highly dependent on the crustal structure, especially for nearby stations. Errors introduced by the station operators' incorrect readings of the first motion polarity or misidentification of body wave phases were minimized by direct readings of WWSSN station records whenever possible.

The second method used in this study involves analysis of radiation patterns generated by Rayleigh waves. The amplitude of Rayleigh waves recorded at a particular station is a function of fault geometry and azimuth of the station relative to the epicenter.

The procedure requires first digitizing the long-period analog Rayleigh waves recorded at each station. The digitized data is then Fourier transformed from the time domain to the frequency domain. A range of frequencies is "windowed" (isolated) so that the spectral amplitude of a particular frequency may be observed for all stations. All stations do not lie at equal distances from earthquake, nor do the stations record at equal amplification, so that these spectral amplitudes must be normalized for both distance and amplitude, removing the effects of propagation.

These normalized spectral amplitudes are then plotted as a function of azimuth. The characteristic lobes and nodes of the particular fault geometry are thus produced, although lobes may be somewhat jagged due to noise, and station data in a particular quadrant may be lacking.

Comparisons may then be made of the observed patterns with theoretical patterns which have been generated for various fault geometries.

Rayleigh wave radiation patterns have been used for several events in

this study as a useful supplement to focal mechanism solutions obtained from P-wave polarities.

III. Body Wave Analysis

Body-wave modelling techniques, in which synthetic seismograms are generated and compared to the observed seismogram, provide fairly accurate fault geometry information and serve as a means of constraining focal depths.

The generated seismic rays include the effects of fault geometry, near source velocity structure, and source-receiver separation and consists of theoretical pulses generated at the source and at the interfaces of the velocity structure, scaled for relative amplitudes and time delays.

The synthetic seismogram program used in this study uses the algorithm of Kroeger and Geller (1983). The synthetic seismogram is expressed as a convolution of the form:

$$u(t) = S(t) * NSS(t) * E(t) * RS(t) * I(t)$$

where u(t) is the seismogram, S(t) is the far field source time function of the earthquake, NSS(t) represents the effects of the fault geometry, propagation, and near source structure, and I(t) is the response of the recording instrument. The effects of geometrical spreading, anelastic attenuation, and travel time from the source to receiver are included within E(t).

For shallow continental earthquakes, the major effects of earth structure within the first minute of recording the P wave are pP and sP, due to reflections of upgoing P and S waves at the earth's surface.

Synthetic seismograms are particularly useful in that they allow for the refinement of the near source structure term. This term is a time series of scaled impulses, one for each ray which enters a homogeneous halfspace as a result of interaction with a velocity structure of horizontal layers near the source. S(t) is convolved with NSS(t); this result is then convived with E(t) to yield the ground response.

Convolution of the ground response with I(t) then yields the synthetic seismogram. For the purposes of this study, the near receiver structure, RS(t), has been neglected.

The resultant seismogram is a function of near source crustal structure and the focal depth, which control phase arrival times, and of fault geometry, which controls the amplitudes of the pulses. Thus once a well-constrained focal mechanism solution has been obtained from P-wave and Rayleigh wave data, the focal depth may be approximated. Long period waveforms are much less sensitive to crustal structures and may be approximated by a crustal layer overlying an infinitely thick mantle halfspace. Short period waveforms are much more difficult to model, requiring the manipulation of two unknown parameters, the focal depth and crustal structure.

Event 1 (Mb = 5.9) exhibited long-period waves suitable for modelling, and short period synthetics were modelled for event 2 (Mb = 5.4). An attempt to model waveforms for the event of 72-08-03 proved unsuccessful because of the small amplitude of the waveforms.

Crustal structure for long-period synthetics was approximated using a 33 km thick crustal layer (Vp = 5.5 km/s, Vs = 3.3 km/s, density = 2.9 g/cm**3) overlying an infinitely thick mantle halfspace (Vp = 6.5 km/s, Vs = 3.95 km/s, density = 2.9 g/cm**3).

For short-period synthetics, crustal structure was modelled as follows (from Cook, pers. comm., 1985):

Vp (km/s)	Vs (km/s)	density (g/cm**3)	thickness(km)
3.5	1.25	2.0	0.4
4.6	2.30	2.5	3.6
5.6	3.00	2.7	10.0
5.8	3.50	2.8	20.0
6.5	3.95	2.9	40/000min

APPENDIX B

POLES OF ROTATION CALCULATIONS

Relative plate motions may be described by a rotation of one plate relative to the other about a pole of rotation. If two adjacent plates have a series of faults as a common boundary, then the horizontal projection of slip vectors (hereafter referred to as slip vectors) for these faults must lie on small circles about this pole of rotation. Each pair of adjacent plates will therefore have a corresponding pole of rotation.

If the Okhotsk plate exists, then three separate poles of rotation will lie in northeast Siberia: North America-Eurasia, Eurasia-Okhotsk, and North America-Okhotsk. Otherwise, if the Sea of Okhotsk lies within either the North American or Eurasian plates, then only one pole, the Eurasia-North America pole, will be sufficient to describe the plate motions in northeast Siberia.

The program used for these calculations was adapted from Morgan (1968) and predicts a pole of rotation from the data set in the following manner. A grid encompassing a range of latitude and longitude is created, with the grid step size (increment between successive latitudes and

longitudes) designated by the program user. For each fracture zone or earthquake, the latitude, longitude, azimuth (horizontal projection of the slip vector, for earthquakes) and its uncertainty in degrees of the azimuth are input. For slip vectors, this uncertainty is determined by the quality of the focal mechanism solution.

A hypothetical pole of rotation is then successively placed at each grid position; a line is projected from this pole to the fracture zone or slip vector. The angle between this projected line and the azimuth of the fracture zone or slip vector ideally should be 90°. The program next determines the root mean square residual to measure the misfit between each fracture zone or slip vector azimuth and the hypothetical pole position using the following equations:

SUM1 =
$$\sum_{\text{ERRORAZ}} \frac{\text{FDIST}}{\text{ERRORAZ}} \times (\Delta AZ)^2$$
 SUM2 = $\sum_{\text{ERRORAZ}} \frac{\text{FDIST}}{\text{ERRORAZ}}$

ERROR = (SUM1 / SUM2)

where:

ΔAZ = (azimuth of theoretical slip vector realtive to pole as north pole) - (measured azimuth of slip vector in the same coordinate system)

FDIST = distance form slip vector to pole

ERRORAZ = uncertainty in degrees of measured slip vector azimuth

The minimum least squares error is thus the best fit for the position of the pole of rotation for the data set.

A "confidence ellipse" about the calculated pole of rotation was approximated by including within the ellipse all values of $F = 1.25 * F_{min}$, where F_{min} is the root mean square minimum error obtained from the pole calculations (LePichon et al., 1973).

The data set for which calculations were made consisted of 4 transform faults and 39 horizontal projections of earthquake slip vectors obtained from the north Atlantic to Sakhalin and the Kuril-Aleutian arc-arc junction. These data were then divided into five data sets (Tables B1-B5) in order to determine the pole of rotation for each data set. If two data sets showed nearly the same pole of rotation, then it was assumed that the earthquakes or fracture zones lay along the same boundary. The results for individual data sets are as follows.

Data set 1: North Atlantic to 70°N

The Arctic Mid-Ocean Ridge and its continental extension, the Moma region, are considered by many authors (i.e., Chapman and Solomon, 1976;

Savostin and Karasik, 1981; Churkin, 1972) to represent the Eurasian–North American plate boundary. The best-fitting pole for these data indicate a pole position at 72.15°N, 130.50E, very near the Lena River delta. Table B1 indicates that for this pole, most values of \triangle AZ, which should ideally approximate 0°, are close to 0°. Thus the pole for data set 2 is considered fairly accurate.

Data set 2: Sakhalin only

Chapman and Solomon (1976) have obtained slip vectors for six earthquakes occurring on the island of Sakhalin (Table B2), which they consider as the southern extension of the Eurasian-North American plate boundary. These data alone indicate a pole position at 61.00°N, 130.30°E, very near the Eurasian-North American pole calculated by Chapman and Solomon (1976), using data from the north Atlantic and Sakhalin, of 61.8°N, 130.0°E. The pole calculated in this study for data set 6 is clearly distinct from the pole obtained for data set 2 (the north Atlantic to 70°N). Again \triangle AZ shows values very near 0°.

Data set 3: North Atlantic to Sakhalin

Does Sakhalin lie along the Eurasian-North American plate boundary, or do earthquakes occurring in Sakhalin the result of the interaction between the Okhotsk and Eurasian plates? Combining data from the North Atlantic to Sakhalin (Table B3) the best-fitting pole for this data set lies at 70.00°N, 130.00°E, between the poles calculated for the north Atlantic to 70°N and the Sakhalin data sets. The difference between values of \triangle AZ for this data set and the Sakhalin data set show an increase of about 10° for each data point. \triangle AZ values for this data set and the north Atlantic-70°N data set show only a 3° difference. This suggests that the minimum for this pole at 70.00°N, 130.00°E is influenced more by the data set of the north Atlantic to 70°N, and that Sakhalin does not lie along the Eurasian-North American plate boundary.

Data set 4: 68 N to Kuril-Aleutian arc-arc junction

Do earthquakes along the northeastern Sea of Okhotsk represent interaction between the Eurasian and North American plates, or is there a separate Okhotsk plate? If the former is true, then the combined two data sets (north Atlantic to 70°N and 68°N to Kuril-Aleutian arc-arc junction)

should have the same pole of rotation.

Events in this region, with the exception of the three events in the southern Cherskiy Mountains, are poorly constrained; values of ERRORAZ (the uncertainty in degrees of slip vector azimuth) ranged from 5–25°. It must be noted that ERRORAZ does not allow the azimuth of the slip vector to rotate for each calculations, it only decreases the error associated with the calculations for a particular pole position. For such high values of ERRORAZ in the data set, the pole position will thus be greater influenced by the better constrained slip vector azimuths.

The best-fitting pole for this data set lies at 69.00°N, 158.00°E, much further east than the poles predicted for Sakhalin or for the north Atlantic to 70°N. Observing values of \triangle AZ (Table B4), it is apparent that this pole is most likely constrained by the events in the Cherskiy Mountains. In an attempt to determine whether the pole position would vary if all slip vectors for this data set were equal, the calculations were repeated with ERRORAZ = 5.0 for all data points. The effect was to move the pole position 1°W and increase the least squares value (the minimum). Thus this pole position, while poorly constrained, may be considered to be fairly accurate.

Data set 5: North Atlantic to Kuril-Aleutian arc-arc junction

The calculations for the combined data sets (north Atlantic to 70°N and 68°N to Kuril-Aleutian arc-arc junction) indicate a pole at 67.50°N, $144.00^{\circ}E$, between the poles calculated for the separate data sets.

Observing values of $\triangle AZ$ (Table B5) for this pole position shows that the fit to the data north of 70°N is very good, while the fit to the data is very poor south of 70°N. Thus, this pole position was most likely influenced by the data set from the north Atlantic to 70°N.

Is there a separate Okhotsk plate? This study implies that there are indeed three separate poles of rotation in northeast Siberia: the Eurasia-North America (72.15°N, 130.50°E), the North America-Okhotsk (69.00°N, 158.00°E), and the Eurasia-Okhotsk (61.00°N, 130.30°E) poles; the poles are for enough removed from one another to be considered separate. The results of these calculations do indeed indicate that there exists a separate Okhotsk plate.

DATA SETS FOR POLES OF ROTATION CALCULATIONS

Table B1: DATA SET 1 - North Atlantic to 70N

Pole at 72.15N, 130.50E

NUM	DATE	LAT	LONG	AZ*	ERRORAZ**	SOUR CE#	△ AZ##
40	T	79.00N	2.50E	1 28	10	8	4.64
41	T	71.00N	-8.00E	115	5	8	3.92
42	T	66.50N	-20.00E	98	10	8	-5.59
44	T	50.52N	-33.50E	95	3	8	-0.93
45		79.80N	2.60E	137	10	8	12.65
46		79.80N	2.40E	133	10	8	8.78
47		80.20N	-1.00E	128	10	8	5.63
48		70.90N	-7.60E	115	10	8	3.77
49		66.70N	-18.20E	115	10	8	10.53
50	1963-03-28	66.30N	-19.80E	107	10	8	3.37
51	1967-02-13	52.80N	-34.30E	95	10	8	-0.66
1	1976-09-16	84.30N	0.90E	135	5	3	5.74
2	1973-11-09	86.05N	32.80E	163	5	3	2.33
3	1964-07-31	86.47N	40.70E	177	13	4	7.63
4	1968-06-08	87.00N	51.40E	8	7	4	-6.46
5	1975-03-02	85.01N	98.00E	185	13	4	51.70
6	1975-02-26	84.98N	98.50E	35	5	3	12.24
8	1970-04-23	80.65N	122.00E	64	10	4	-43.41
9	1964-08-25	78.15N	126.65E	67	5	3 3	-45.37
11	1969-04-07	76.55N	130.86E	72	7	3	-19.44
12	1983-06-10	75.33N	127.26E	39	5	3	-8.53
13	1964-07-21	72.10N	130.10E	35	5	2	-57.35
14	1980-02-01	73.06N	122.59E	5	7	2 2	12.24
15	1963-05-20	72.20N	126.25E	168	7	2	-11.82
16	1975-08-12	70.76N	127.12E	18	10	2	-71.88

T = TRANSFORM FAULT

SOUR CE

^{*} AZ = AZIMUTH OF HORIZONTAL PROJECTION OF SLIP VECTOR

^{**} ERRORAZ = VARIANCE IN DEGREES OD SLIP VECTOR AZIMUTH

^{##} $\triangle AZ = (AZIMUTH OF THEORETICAL SLIP VECTOR WITH POLE AS NORTH POLE) - (MEASURED AZIMUTH OF SLIP VECTOR)$

^{1.} MCMULLEN, 1985

^{2.} COOK ET AL., 1985

^{3.} JEMSEK ET AL., 1983

^{4.} SAVOSTIN AND KARASIK, 1981

^{5.} LAZAREVA AND MISHARINA, 1965

^{6.} CORMIER, 1975

^{7.} CHAPMAN AND SOLOMON, 1976

^{8.} MINSTER AND JORDAN, 1978

Table B2: DATA SET 2 - Sakhalin

Pole at 61.00N, 130.30E

NUM	DATE	LAT	LONG	AZ*	ERRORAZ**	SOUR CE#	∆ AZ##
60 61 62 63 64 65	1964-10-02 1971-09-05 1971-09-08 1971-09-08 1971-09-27 1970-01-20	51.95N 46.54N 46.44N 46.28N 46.41N 42.48N	142.92E 141.15E 141.09E 141.03E 141.16E 143.04E	58 77 70 67 74 69	10 10 10 10 10	7 7 7 7 7 7	0.29 6.49 -1.62 -3.89 3.53 -2.86

(SEE TABLE B1 FOR KEY)

Table B3: DATA SET 3 - North Atlantic to Sakhalin

Pole at 70.00N, 130.00	0 E
------------------------	-----

NUM	DATE	LAT	LONG	AZ*	ERRORAZ**	SOUR CE#	△ AZ##
40	T	79.00N	2.50E	1 28	10	8	2.73
41	T	71.00N	-8.00E	115	5	8	2.27
42	T	66.50N	-20.00E	98	10	8	-6.82
44	T	50.52N	-33.50E	95	3	8	-1.66
45		79.80N	2.60E	137	10	8	10.77
46		79.80N	2.40E	133	10	8	6.91
47		80.20N	-1.00E	128	10	8	3.89
48		70.90N	-7.60E	115	10	8	- 2.11
49		66.70N	-18.20E	115	10	8	9.24
50	1963-03-28	66.30N	-19.80E	107	10	8	2.14
51	1967-02-13	52.80N	-34.30E	95	10	· 8	-1.36
1	1976-09-16	84.30N	0.90E	135	5	3	4.24
2	1973-11-09	86.05N	32.80E	163	5	3	0.58
3	1964-07-31	86.47N	40.70E	177	13	4	5.92
4	1968-06-08	87.00N	51.40E	8	7	4	-4.87
5	1975-03-02	85.01N	98.00E	185	13	4	53.82
6	1975-02-26	84.98N	98.50E	35	5	3	14.37
8	1970-04-23	80.65N	122.00E	64	10	4	-40.69
9	1964-08-25	78.15N	126.65E	67	5	3	-31.06
11	1969-04-07	76.55พ	130.86E	72	7	3	20.58
12	1983-06-10	75.33N	127.26E	39	5	3	-61.20
13	1964-07-21	72.10N	130.10E	35	5	2	-55.93
14	1980-02-01	73.06N	122.59E	5	7	2	43.95
15	1963-05-20	72.20N	126.25E	168	7	2	47.31
16	1975-08-12	70.76N	127.12E	18	10	2	18.80
60	1964-10-02	51.95N	142.92E	58	10	7	-18.48
61	1971-09-05	46.54N	141.15E	77	10	7	-3.73
62	1971-09-08	46.44N	141.09E	70	10	7	-10.77
63	1971-09-08	46.28N	141.03E	67	10	7	-13.88
64	1971-09-27	46.41N	141.16E	74	10	7	-6.69
65	1970-01-20	42.48N	143.04E	69	10	7	-11.66

(SEE TABLE B1 FOR KEY)

Table B4:Data Set4 - 68N to Kuril-Aleutian arc-arc junction

Pole at 69.0N, 158.0E

NUM	DATE	LAT	LONG	AZ*	ERRORAZ**	SOURCE#	△ A2##
18	1976-01-21	67.70N	140.00E	4	13	2	-23.36
20	1968-09-09	66.20N	141.10E	148	5	2	-0.83
21	1971-05-18	63.92N	146.10E	122	5	1	-5.74
22	1970-06-05	63.26N	146.18E	130	5	1	5.50
23	1972-01-13	61.94N	147.40E	99	5	1	-18.19
25	1981-05-22	61.09N	156.68E	60	25	1	-33.33
26	1979-08-19	61.33N	159.12E	79	20	1	-8.00
28	1978-06-05	60.09N	160.35E	35	25	1	-49.59
29	1972-08-03	59.51N	163.10E	104	20	1	-24.59
31	1976-01-21	58.93N	163.57E	34	20	1	-44.84
34	1969-11-22	57.76N	163.54E	130	15	6	-49.99
37	1969-12-23	57.32N	163.40E	103	20	6	-22.40

(SEE TABLE B1 FOR KEY)

Table B5: DATA SET 5 - North Atlantic to Kuril-Aleutian arc-arc junction

Pole at 67.50N, 144.00E

NUM	DATE	LAT	LONG	AZ*	ERRORAZ**	SOUR CE#	△ AZ##
40	T	79.00N	2.50E	128	10	8	11.13
41	T	71.00N	-8.00E	115	5	8	8.85
42	T	66.50N	-20.00E	98	10	8	1.50
44	T	50.52N	-33.50E	95	3	8	3.90
45		79.80N	2.60E	137	10	8	19.47
46		79.80N	2.40E	133	10	8	15.61
47		80.20N	-1.00E	128	10	8	12.79
48		70.90N	-7.60E	115	10	8	8.65
49		66.70N	-18.20E	115	10	8	15.51
50	1963-03-28	66.30N	-19.80E	107	10	8	8.42
51	1967-02-13	52.80N	-34.30E	95	10	8	4.25
1	1976-09-16	84.30N	0.90E	135	5	3	14.89
2	1973-11-09	86.05N	32.80E	163	5	3	12.48
3	1964-07-31	86.47N	40.70E	177	13	4	18.24
4	1968-06-08	87.00N	51.40E	8	7	4	1.75
5	1975-03-02	85.01N	98.00E	185	13	4	38.83
6	1975-02-26	84.98N	98.50E	35	5	3	-0.68
8	1970-04-23	80.65N	122.00E	64	10	4	-61.63
9	1964-08-25	78.15N	126.65E	67	5	3	-57.22
11	1969-04-07	76.55N	130.86E	72	7	3	-48.52
12	1983-06-10	75.33N	127.26E	39	5	3	8.56
13	1964-07-21	72.10N	130.10E	35	5	2	2.10
14	1980-02-01	73.06N	122.59E	5	7	2	22.15
15	1963-05-20	72.20N	126.25E	168	7	2	16.97
16	1975-08-12	70.76N	127.12E	18	10	2	2.39
18	1976-01-21	67.70N	140.00E	4	13	2	1.62
20	1968-09-09	66.20N	141.10E	1 48	5	2	18.08
21	1971-05-18	63.92N	146.10E	122	5	1	-44.61
22	1970-06-05	63.26N	146.18E	130	5	1	-51.10
23	1972-01-13	61.94N	147.40E	99	5	1	-22.11
25	1981-05-22	61.09N	156.68E	60	25	1	5.03
26	1979-08-19	61.33N	159.12E	79	20	1	28.97
28	1978-06-05	60.09N	160.35E	35	25	1	-17.89
29	1972-08-03	59.51N	163.10E	104	20	1	-52.55
31	1976-01-21	58.93N	163.57E	34	20	1	-18.65
34	1969-11-22	57.76N	163.54E	130	15	6	-74.27
37	1969-12-23	57.32N	163.40E	103	20	6	-46.09

LIST OF REFERENCES

- Akademiya Nauk SSSR, Zemletryaseniya SSSR, 1964-1981, Izdatel'stvo "Nauka", Moskva.
- Akademiya Nauk SSSR, Operativnyi Seismologicheskii Byulleten' (ezhedekadnyi), 1980-1983, Mezhduvedomstvehnyi Geotizicheskii Komitet, Moskva.
- Akademiya Nauk SSSR, Seismologicheskii Byulleten (ezhedekadnyi), 1983-1984, Obninsk.
- Afanasenko, V.Y., and Naymark, A.A., 1978, Naled formation and neotectonics of the Moma rift region (northeast USSR): Int. Geol. Rev., v. 20, p.167-176.
- Aver'yanova, V.N., 1973, Seismic Foci in the Far East: Israel Program for Scientific Translations, Jerusalem, Israel, 207 p.
- Chapman, M.E., and Solomon, S.C., 1976, North American Eurasian plate boundary in northeast Asia: J. Geophys. Res., v. 81, p. 921-930.
- Churkin, M., Jr., 1972, Western boundary of the North American continental plate in Asia: Geol. Soc. Am. Bull., v. 83, p. 1027–1036.
- Cook, D.B.; Fujita, K.; and McMullen, C.A., 1984, Seismotectonics of northern Yakutia and the Laptev Sea, Eos, v. 65, p. 1016.
- Cormier, V.F., 1975, Tectonics near the junction of the Aleutian and Kurile-Kamchatka arcs and a mechanism for Middle-Tertiary magmatism in the Kamchatka Basin: Geol. Soc. Am. Bull., v. 86, p. 443-453.
- Creager, K.C., and Jordan, T.H., 1984, Slab penetration into the lower mantle: J. Geophys. Res., v. 89, p. 3031-3049.

- Dickinson, W.R, and Seely, D.R., 1979, Structure and stratigraphy of forearc regions: Amer. Assoc. Pet. Geol. Bull., v. 63, p. 2-31.
- Den, N., and Hotta, H., 1973, Seismic refraction and reflection evidence supporting plate tectonics in Hokkaido: Pap. Meteorol. Geophys., v. 24, p. 31-51.
- Fedotov, S.A.; Simbireva, I.G.; Feodilaktov, V.D.; and Matvienko, Y.D., 1980, Zemletryaseniya Kamchatki, <u>in</u> Zemletryaseniya v SSSR v 1976 godu: Izdatel'stvo Nauka, Moskva, USSR, p. 83-87.
- Filson, J., and Frasier, C.W., 1972, The source of a Siberian Earthquake: Eos, v. 53, p. 1041.
- Fujita, K., 1978, Pre-Cenozoic tectonic evolution of northeast Siberia: J. Geol., v. 86, p. 159-172.
- Fujita, K., 1979, Tectonics of divergent and convergent plate margins: Ph. D. Dissertation, Northwestern University, Evanston, 300 p.
- Fujita, K., and Newberry, J.T., 1983, Accretionary terranes and tectonic evolution of Northeast Siberia, in Accretionary Terranes in the Circum-Pacific Regions, eds. M. Hashimito and S. Uyeda, Terra Scientific Publishing Co., Tokyo, p. 43-57.
- Gutenburg, B., and Richter, C.F., 1954, Seismicity of the Earth and Associated Phenomena: Hafner Publishing Co., New York, 310 p. (reprint, 1965)
- Herrin, E.; Arnold, E.P.; Bolt, B.A.; Clawson, G.E.; Engdahl, E.R.; Freedman, H.W.; Gordon, D.W.; Hales, A.L.; Lobdell, J.L.; Nuttli, O.; Romney, C.; Taggart, J.; and Tucker, W., 1968: 1968 seismological tables for P phases: Bull. Seismol. Soc. Am., v. 58, p. 1193-1241.
- International Seismological Center, Regional Catalog of Earthquakes, v. 1-19, Edinburgh, Scotland, 1964-1982.
- International Seismological Summary, Edinburgh, Scotland, 1913-1963.

- Jeffries, H., and Bullen, K.E., 1940, Seismological Tables: British Assoc. of the Advancement of Science, London (reprint, 1970)
- Jemsek, J.P.; Bergman, E.A.; Nabelek, J.L.; and Solomon, S.C., 1984, Focal depths and mechanisms of large earthquakes on the Mid-Arctic ridge system: Eos, v. 65, p. 273.
- Kondorskaya, N.V., and Shebalin, N.V., 1982, New Catalog of Strong Earthquakes in the USSR from Ancient Times through 1977: World Data Center for Solid Earth Geophysics, Report SE-31, 597 p.
- Koz'min, B.M., 1973, Zemletryaseniya Yakutii; <u>in</u> Zemletryaseniya v SSSR v 1970 godu: Izdatel'stvo "Nauka", Moskva, USSR, p. 147-154.
- Koz'min, B.M.; Emel'yanov, N.P.; Emel'yanova, A.A.; Zhelinskaya, E.A.; Larionov, A.G.; and Li, B.F., 1975, Sil'nye Zemletryaseniya Yakutii in Zemletryaseniya SSSR 1971 godu: Izdatel'stvo "Nauka", Moskva, p. 133-141.
- Koz'min, B.M., 1984, Seismicheskie Poyasa Yakutii i Mekhanizmy Ochagov ikh Zemletryasenii: Izdatel'stvo "Nauka", Moskva, 126 pp.
- Kroeger, G.C., and Geller, R.J., 1983, An efficient method for computing synthetic reflection seismograms for plane layered models: Eos, v. 64, p. 772.
- Lazareva, A.P., and Misharina, L.A., 1965, Stresses in earthquake foci in the Artic seismic belt: Izvestiya Academy of Sciences of the USSR, Phys. Solid Earth, v. 1, p. 84-87.
- LePichon, X.; Francheteau, J.; and Bonnin, j., 1973, Plate Tectonics, Elsevier Scientific Publishing Co., Amsterdam.
- Leonenko, N.A., 1975, Structural zonation of Taygonos Peninsula: Int. Geol. Rev., v. 18, p. 640-646.
- Minster, J.B., and Jordan, T.H., 1978, Present day plate motions: J. Geophys. Res., v. 83, p. 5331-5354.

- Molnar, P.; Fitch, T.J.; and Wu, F.T., 1973, Fault plane solutions of shallow earthquakes: Earth Planet. Sci. Lett., v. 19, p. 101-112.
- Morgan, W.J., 1968, Rises, trenches, great faults, and crustal blocks, J. Geophys. Res., v. 73, p. 1959-1982.
- Naymark, A.A., 1976, Neotectonics of the Moma region, northeastern USSR: Acad. Sci. USSR, Dokl., Earth Sci. Sect., v. 229, p. 39-42.
- Newberry, J.T., 1983, A Detailed study of seismicity, earthquake mechanisms, and depth phases in the far western Aleutians: M.S. Thesis, Michigan State University, East Lansing, 93 pp.
- Parfenov,L.M.; Voinova, I.P.; Natal'in, B.A.; and Semenov, D.F., 1978, Geodynamics of the northeastern Asia in Mesozoic and Cenozoic time and the nature of volcanic belts: J. Phys. Earth, v. 26, Suppl., p. 5503–5525.
- Pho, H.T., and Behe, L., 1972, Extended distances and angles of incidence of P waves; Bull. Seismol. Soc. Amer., v. 62, p. 885-902.
- U.S. Department of the Interior/Geological Survey, Preliminary Determination of Epicenters, National Earthquake Information Service, Washington, D.C., 1980-1983.
- Rezanov, I. A., and Kochetkov, V. M., 1962, Recent tectonics and seismic regionalization in the northeastern region of the USSR, Acad. Sci. USSR, Izvestiya, Geophys. Ser., p. 1673-1674.
- Rothé, J.P., 1969, Seismicity of the Earth: United Nations Educational Scientific and Cultural Organization, Paris, 336 pp.
- Savostin, L.A., and Karasik, A.M., 1981, Recent plate tectonics of the Arctic Basin and of northeastern Asia: Tectonophys., v. 74, p. 111-145.
- Savostin, L.A.; Verzhibtskaya, A.I.; and Baranov, B.V., 1982, Holocene plate tectonics of the Sea of Okhotsk region: Acad. Sci. USSR, Doklady, Earth Sci. Sect., v. 226, p. 961-965.

- Savostin, L.; Zonenshain, L.; and Baranov, B., 1983, Geology and plate tectonics of the Sea of Okhotsk: Geodynamic series, Amer. Geophys. Union, v. 11, p. 189-222.
- Scholl, D.W.; Buffington, E.C.; and Marlow, M.S., 1975, Plate tectonics and the structural evolution of the Aleutian-Bering Sea region; Geol. Soc. Am., Spec. Pap. 151, p. 1-31.
- Shapiro, M.I., 1976, Northeastern continuation of the east Kamchatka synclinorium; Geotectonics, v. 10, p. 76-78.
- Stauder, W., and Mualchin, L., 1976, Fault motion in the larger earthquakes of the Kurile-Kamchatka arc and of the Kurile-Hokkaido corner: J. Geophys. Res., v. 81, p. 297-308.
- Udias, A., and Stauder, W., 1964, Application of numerical methods for S-wave focal mechanism determinations to earthquakes of the Kamchatka-Kurile Islands region: Bull. Seismol. Soc. Amer., v. 54, p. 2049-2065.
- Ufimtsev, G.F., 1975, Neotectonics of the continental part of the Soviet far east: Acad. Sci. USSR, Doklady, Earth Sciences Sections, v. 221, p. 111-113.
- Veith, K.F., 1974, The Relationship of Island Arc Seismicity to Plate Tectonics: Ph.D. dissertation, Southern Methodist University, Dallas.
- Watson, B.F., 1985, The tectonic evolution of Kamchatka peninsula, USSR, M.S. Thesis, Michigan State University, East Lansing.
- Watson, B.F., and Fujita, K., 1985, Tectonic evolution of Kamchatka and the Sea of Okhotsk and implicattions for the Pacific Basin, <u>in</u>

 Proceedings of Circum-Pacific Tectonostratigraphic Terrane

 Symposium, ed. Howell, D.G, Circum-Pacific Energy and Mineral Resources Council, Tulsa.
- Yermakov, B.V.; Bazhenova, O.K.; and Burlin, Yu. K., 1975, Oil and gas potential of the Komandor Basin: Acad. Sci. USSR, Doklady, Earth Sci. Sect., v. 220, p.99-101.

Zobin, V.M., and Simbireva, I.G., 1977, Focal mechanisms of earthquakes in Kamchatka – Commandor region and heterogeneity of the active seismic zone: Pure and Appl. Geophys., v. 15, p. 284–299.